Serially Connected Forward Osmosis Membrane Elements of Pressure-assisted Forward Osmosis-Reverse Osmosis Hybrid System: Process Performance and Economic Analysis

Seungho Kook[a], Chulmin Lee[a], Nguyen Thanh Tin[a], Jangho Lee[a], Ho Kyong Shon[b], In S. Kim[a,c*]

[a] *School of Earth Sciences and Environmental Engineering, Gwangju Institute of Science and Technology (GIST), 123 Cheomdangwagi-ro, Buk-gu, Gwangju 61005, South Korea*

[b] *Centre for Technology in Water and Wastewater, School of Civil and Environmental Engineering, University of Technology Sydney (UTS), P.O. Box 123, 15 Broadway, NSW2007, Australia*

[c] *Global Desalination Research Center, Gwangju Institute of Science and Technology (GIST), 123 Cheomdanwagi-ro, Buk-gu, Gwangju 61005, South Korea*

ABSTRACT

Pressure-assisted forward osmosis (PAFO) has been considered an alternative of forward osmosis (FO) process to reduce capital expenditure (CAPEX) of FO. This is mainly attributed to the enhanced water flux through the FO membranes which leads to the improved dilution of draw streams. In this regard, it has been expected that employing PAFO in the FO – reverse osmosis (RO) hybrid system for seawater desalination can reduce the overall economics of the hybrid process. However, replacing FO with PAFO causes an additional energy cost in the seawater dilution step which inevitably leads to a question that PAFO-RO hybrid is truly an economically beneficial option over FO-RO and stand-alone RO desalination. More importantly, though serial connection of FO elements (SE) improves the dilution of initial draw water which can induce enhanced energy cost saving in the following RO step, this economic benefit is also compensated with the additional membrane cost in the PAFO unit process.

To rationalize its overall performance and economic benefit, the thorough performance and economic evaluation were conducted based on actual pilot-scale PAFO operations for serial connection of three 8040 FO elements(SE1, SE2 and SE3). A scenario was assumed that PAFO is implemented as an additional pretreatment step of existing RO process. The results showed that the FO-RO hybrid process is not an economically feasible option unless a significant unit FO element cost cut-down is guaranteed. On the other hand, PAFO-RO hybrid showed some benefits with regards to a higher range of target RO recovery and unit FO element cost, particularly when two FO elements are serially connected (SE2). However, consideration on overall plant construction and operating cost components led to a conclusion that the skepticism on the hybrid process has to be maintained. This skepticism can be alleviated when a new PAFO-RO hybrid desalination plant is commissioned primarily due to significant potential CAPEX and OPEX savings in the RO process originated from the significant reduction of

seawater intake.

Highlights

- Significant impact of initial draw flowrate and hydraulic pressure on the economics of PAFO in hybridization with RO
- Hydraulic pressure dependence of FO membrane element performance
- Drastic pressure-drop in the draw channel of the last element in serial configuration
- Target RO recovery and FO element cost in PAFO-RO hybrid are important for economics

Keywords: Forward osmosis (FO); Pressure assisted-forward osmosis (PAFO); Serial configuration; Economic feasibility; Desalination

1. Introduction

To alleviate the water scarcity issue in global scale, forward osmosis (FO) process was introduced [1] and has been widely acknowledged in and out of academia as one of the promising desalination technologies that can potentially replace seawater reverse osmosis (SWRO) process. Utilizing osmotic pressure as the major driving force for water transport, this direct osmosis process requires significantly low amount of electricity as a unit process compared to conventional SWRO processes [2]. In the early stage of FO studies in the last decade, seawater as feed water source has been widely adopted as means of replacing RO [1, 3, 4]. These efforts, however, came to an end when a fundamental thermodynamic drawback became problematic for the FO process as a means of stand-alone FO seawater desalination requires higher energy in the following water retrieving process than the conventional RO [reference]. To eliminate this flaw in a practical application, FO has been suggested as a pretreatment measure for RO (i.e. serving as a unit process for seawater dilution by utilizing impaired water sources as feed and seawater as draw), namely FO-RO hybrid process [5]. For electricity cost is the major component of operating expenditure (OPEX) of RO [6], employing diluted seawater guided to the following RO naturally leads to the energy cost saving as opposed to the conventional RO, thereby potentially leading to overall plant cost reduction. Nevertheless, the economics of the hybrid process has not been clearly validated since additional capital expenditure (CAPEX) of FO can be significant enough to make the economics of the hybrid scheme not feasible.

Pressure-assisted forward osmosis (PAFO) has been studied in recent years to enhance the draw stream dilution by applying moderate hydraulic pressure to the feed side [7-10]. This potentially leads to further energy cost reduction in the PAFO-RO hybrid system. This approach, however, embraces both benefits and disadvantages; enhanced dilution by PAFO surely reduces the energy cost of RO and FO membrane cost. However the additional energy cost for pressurizing the feed stream in the FO unit process can be a critical component of the operating expenditure. In this context, such a controversial hybrid process necessitates a thorough economic assessment considering the pros and cons based on actual pilot-scale testing.

As the number of FO elements serially connected increases, further dilution can be expected, though with uncertainties of the serial connection in the overall economics. There have been other attempts to evaluate the economic feasibility of the FO-RO hybrid, yet, with a limitation that the data sets were drawn from lab-scale tests employing small membrane coupons [8, 11]. Unlike previously reported FO performance in lab-scale tests, it has been reported that the actual FO element performances in pilot-scale tests are strongly dependent on hydraulic pressure [12-15]. They found that, if the membranes are serially connected, a significant pressure build-up at the inlet (particularly in the draw inlet) arises [12]. This is a direct indication that the economics of PAFO-RO hybrid process is in close relation with the hydraulic pressure dependence of FO elements in series. A recent economic evaluation was employed with single element-based pilot-scale test using an 8-inch FO membrane element. They observed that the economics can be affected by hydraulic pressure dependence [16]. However, such a simulated hydraulic pressure dependence derived from single element-based results may underestimate the electricity cost of PAFO since serially connected FO elements require higher inlet pressure to accommodate equivalent initial flowrate to that of the single element case as discussed above. In addition, contraction of a draw channel dependent on operating factors such as flowrate and pressure [17] can be a crucial determining factor for accurate projection of data sets to the economics.

Therefore, economic analysis by actual serial connection of FO elements improves the validity and reliability of the economic feasibility of PAFO-RO hybrid. Accordingly, the objective of this study is to evaluate the economics of PAFO-RO hybrid by focusing on the hydraulic pressure dependence of the FO element performance. For the economic assessment, a scenario was assumed that the PAFO process was used as pretreatment to an existing full-scale conventional 2-stage RO plant.

2. Materials and methods

2.1. Pilot-scale PAFO operation

2.1.1. FO element

Spiral-wound FO element (CSM FO-8040, Toray Chemical Korea Inc., Korea) was used for pilot-scale testing. The FO element consists of 12 layers of membrane leaves that include two polyamide thin-film composite (PA-TFC) flat sheet membranes, two layers of tricot fine spacers and a diamond-shaped spacer in the center enveloped by the two fine spacers. Total effective membrane area of the element was 15.3 m^2. Detailed description of the characteristics of the membrane can be found elsewhere [18-20]. Also, illustration of the structural characteristics of the element is shown in Fig. 1.

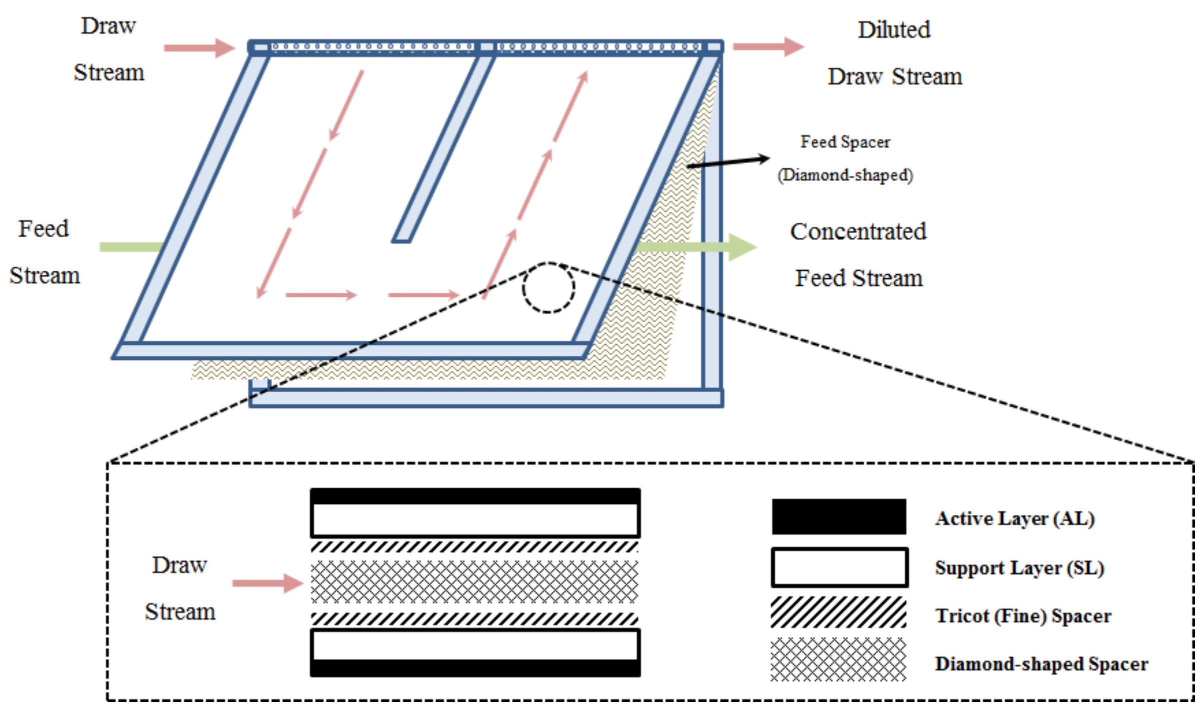

Fig. 1. Structural characteristics of a spiral-wound FO element and the spacer configurations of the membrane leaves of CSM FO-8040

2.1.2. PAFO pilot system and operating conditions

Fig. 2 shows the schematic diagram of the PAFO pilot system. The system was equipped with a feed pump (Grundfos, Product: CRN10-14 A-FGJ-G-E-HQQE, Motor: MG160MB2-42FF300-H3, Denmark) and a draw pump (Grundfos, Product: CRN3-5 A-FGJ-G-E-HQQE, Motor: MG80A2-19FT100-H3, Denmark) and their maximum operating pressures were 21 bar and 5 bar, respectively. Up to three FO elements were installed (one element in one vessel) into the FO pressure vessels (ROPV, R8040B300S-1W 1D5D, maximum pressure = 21 bar, China) and the vessels were serially connected. Digital flowmeters (Endress+Hauser, PROMAG 10, Switzerland), pressure gauges (Endress+Hauser, Cerabar S, Switzerland) and TDS meters (Georg Fischer, Signet 9900 Transmitter, Switzerland) were installed between the pressure vessels and their inlets and outlets to monitor the variations of the major dependent variables (i.e. flowrate, hydraulic pressure and concentration). Data sets were obtained every minute *via* the automated data acquisition system.

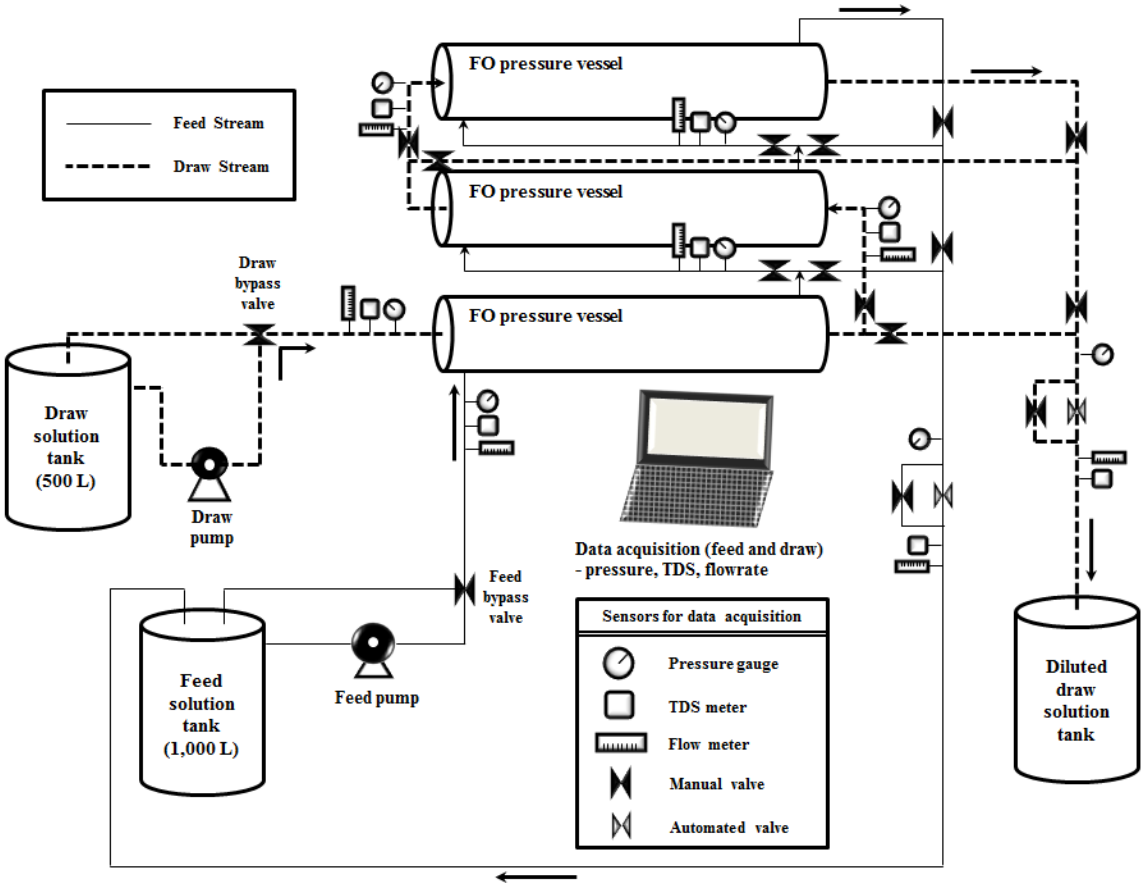

Fig. 2. Process flow diagram of the PAFO pilot system

Initial feed flowrates ($Q_{F,in}$) varied from 50 to 70 L/min and 5 – 7 L/min for initial draw flowrates ($Q_{D,in}$). A set of a manual valve and an automated valve was installed at the final outlet of the respective feed and draw pipeline for accurate control of the two streams. All manual valves depicted in Fig. 2 were adjusted for desired serial connection of FO elements. To ensure safety and prevent the membrane leaves from rupturing during PAFO operations, hydraulic pressure difference between the feed and draw channels was defined as the pressure difference between the feed outlet and the draw inlet of the last element (denoted as ΔP_{serial}) in all serial configurations. Initial feed and draw volumes were 1,000 L and 500 L, respectively. The draw stream was not circulated to ensure that the osmotic pressure of the initial draw stream remained constant and the diluted draw stream was collected in a separate container.

Water flux remained consistent (standard deviation of ± 0.2 LMH) due to the non-circulating draw stream as discussed in our previous study [14]. 5 M NaCl solution was generated and diluted with tap water to match the initial draw concentration ($C_{D,in}$) of 35,000 mg/L TDS. Initial feed concentration ($C_{F,in}$) was set at 200 mg/L TDS. Detailed operating conditions were summarized in Table 1.

Table 1. Summary of operating conditions for pilot-scale PAFO operations

Operational Factors		**Description**	**Note**
Membrane element		CSM FO8040	Toray Chemical Korea, Inc.
Effective membrane area		15.3 m^2	One element
Initial Solutions	Feed, $C_{F,in}$	200 mg/L TDS (500 L)	
	Draw, $C_{D,in}$	35,000 mg/L TDS (1,000 L)	NaCl (99.5% Purity, OCI, Korea)
Initial Flowrates	Feed, $Q_{F,in}$	50, 60, 70 L/min	
	Draw, $Q_{D,in}$	5, 6, 7 L/min	
Pressure Difference, ΔP_{serial}		0, 1, 2, 3, 4 bar (± 0.02 bar)	ΔP_{serial} = feed outlet pressure of the last element – draw inlet pressure of the last element
Serial Connection, SE		1, 2, 3	SE : number of FO elements in series
Temperature		25 ± 1 ºC	
Operation Time		30 min	

Inlet pressures of the lead element for both feed ($P_{F,in}$) and draw ($P_{D,in}$) channels and the diluted draw concentrations ($C_{D,out}$) of the last elements served as the key input variables for the following economic assessments. Some experimental conditions for SE2 and SE3 cases (i.e. 3 and 4 bar for SE2 and 2, 3 and 4 bar for SE3), that the draw inlet pressure exceeded the maximum operating pressure of the draw pump (i.e. 4.6 bar), could not be conducted since $Q_{D,in}$ specified in Table1 could not be achieved (i.e. lower initial draw flowrate).

2.2. Assumptions for economic evaluation

2.2.1. General assumptions

Secondary wastewater effluent was assumed to be the feed source for PAFO and UF pretreated RO seawater was postulated to serve as the draw stream. Unit electricity cost (E_C) was set at 0.1 $/kWh [15]. Daily operation time (t_{op}) was set at 24 h and the design period (DP) was assumed to be 20 years. For amortization of CAPEX components, interest rate was set at 0.06. The final products of the stand-alone 2-stage RO as well as the PAFO-RO hybrid processes were fixed at 100,000 m^3/d. Table S1 summarizes general assumptions and important conditions of RO simulations by ROSA9 software for the economic evaluation.

2.2.2. Assumptions for 2-stage RO

The CAPEX of the full-scale RO process ($CAPEX_{RO}$) was assumed to be constant for this study aims to validate the potential impact of implementation of PAFO to an existing RO plant on economic benefits in terms of RO energy cost reduction. For the specified target final product, $CAPEX_{RO}$ breakdown (Fig. S1a) was estimated from the CAPEX estimator provided elsewhere [6]. The specified cost estimates of the $CAPEX_{RO}$ components were further elaborated in a later section for a strategic approach for improving the economics of the hybridization.

As widely noted, the hybridization of FO with RO is expected to reduce the OPEX of the RO process ($OPEX_{RO}$) due to the dilution of seawater. Replacing FO with PAFO can further reduce the $OPEX_{RO}$ because of the enhanced dilution of draw stream. The simulation results on RO performance with varying feed concentrations were reported in our previous study [14]. Based on the results, the optimal recovery of the stand-alone 2-stage RO process for feed concentration of 35,000 mg/L TDS was set at 55% with the corresponding RO SEC ($SEC_{RO,ROSA}$) of 3.84 kWh/m^3. This fixed SEC_{RO} value served as the basis of evaluating economic benefits in terms of energy cost reduction induced by the hybridization of PAFO and RO.

As illustrated in the $OPEX_{RO}$ breakdown [6] (Fig. S1c), 43.0% of the total $OPEX_{RO}$ is allocated for overall plant electricity cost (i.e. not necessarily for the unit RO process only). From an actual RO plant operation report for Sadara Marafiq desalination plant, Saudi Arabia [21], the proportion of the electricity cost for the RO unit process was estimated as 71.3% of the overall electricity cost. The remaining 28.7% included pretreatment (DAF coupled with UF) (12%), water export (5%), HVAC (heating, ventilation and air conditioning) (5%), seawater intake (3%) and post-treatment, utilities and miscellaneous (3.7%). As a result, the electricity cost for unit RO process ($OPEX_{RO,Unit}$) accounts for 30.7% of the overall $OPEX_{RO}$. At this point, it is important to note that the reported $OPEX_{RO}$ breakdown statistics included the impact of energy recovery device (ERD) while SEC estimation by ROSA9 simulation does not consider this contribution. For diluted draw streams, operating hydraulic pressure of RO decreases and this requires the consideration on the efficiency of ERD (η_e). As reported in [22], the ERD efficiency deteriorates as operating hydraulic pressure decreases. Thus, the conversion of $OPEX_{RO,Unit}$ is required for fair comparison with the ROSA9 simulation results. The η_e was set at 0.95 for stand-alone 2-stage RO and an SEC value including the effect of ERD ($SEC_{RO,ERD}$) was computed using the equation given in [23]; the result gives 2.46 kWh/m^3. The ratio between the $SEC_{RO,ROSA}$ and $SEC_{RO,ERD}$ was found as 1.558 and it was defined as the conversion factor (f_{conv}) for fair comparison. Except the $OPEX_{RO,Unit}$ bound to $SEC_{RO,ROSA}$, the cost estimates of the other $OPEX_{RO}$ components were assumed to strictly follow the specified proportions bound to $SEC_{RO,ERD}$ by dividing the cost estimates with f_{conv}. To more simply put, the cost estimates of all $OPEX_{RO}$ components shown in Fig. S1c except $OPEX_{RO,Unit}$ were obtained considering the effect of ERD while $OPEX_{RO,Unit}$ was separately obtained to exclude the effect of ERD from the ROSA9 simulations for fair comparison. Fig. S1d shows the resulting $OPEX_{RO}$ breakdown for 2-stage RO excluding the effect of ERD.

Upon incorporating PAFO to an existing RO process, operating hydraulic pressure decreases and this might accordingly affect the replacements of parts and materials in the long-term. Thus, it was assumed that the cost for parts and materials ($OPEX_{RO,P\text{-}M}$) proportionally decreases according to the change of $SEC_{RO,ROSA}$ due to dilution. Electricity costs for other unit processes ($OPEX_{RO,Others}$), membrane replacement cost and labour were fixed due to uncertainties. To sum up, only affected $OPEX_{RO}$ components within the hybridized system were $OPEX_{RO,Unit}$ and $OPEX_{RO,P\text{-}M}$ in the current study.

2.2.3. Assumptions for PAFO in the hybridization with RO

Since target RO recovery varies as an independent variable for a fixed final product of 100,000 m^3/d, CAPEX and OPEX of PAFO ($CAPEX_{PAFO}$ and $OPEX_{PAFO}$) are strictly dependent on the change of required RO feed flowrate (i.e. diluted draw stream production). There are three major components of $CAPEX_{PAFO}$: membranes, pressure vessels and pumps. The PAFO train is a combination of a PAFO skid and a set of feed and draw pumps responsible for supplying the feed ($Q_{PAFO,F}$) and draw ($Q_{PAFO,D}$) streams to the respective skid. The PAFO skid consists of FO elements and pressure vessels. At this stage, there is a no guideline for determining the maximum number of FO elements per skid due to unavailability of relevant studies on FO skid design in and out of academia. Skid design, in practical terms, may require analysis on headloss and service ability. This is because the skid design can be determined based on feed and draw pump capacities and their differential pressures for a skid and the accessibility of service crews conducting maintenance. If the skid size is too small, piping work may become simpler and accessibility can be optimal, yet with a significant demand on pump installations and maintenance. In the opposite case, uncertainty escalates with appropriate maintenance on elements and pipelines due to complexed piping work for the skid. Though, it has been reported that, for a nanofiltration plant located in Mery sur Oise, Paris, France, 190 pressure vessels were installed per train for a maximum of service pressure of 20 bar [24]. Considering the similarity of PAFO to nanofiltration in practice, the maximum number of vessels per skid was reasonably limited as 200 in this economic assessment.

The feed pump capacity per skid (Q_{FP}) was accordingly assumed as 600 m^3/h considering the initial feed flowrates specified in Table 1. The cost of the feed pump (FP_C) was assumed to be \$10,000 per skid. Draw pump capacity per skid (Q_{DP}) was determined by the ratio between the feed ($Q_{F,intake}$) and draw ($Q_{D,intake}$) intakes (*IFR*) defined in Table S2. Also, the draw pump cost (DP_C) was obtained following the ratio. Variations of target RO recovery determine the required amount of diluted draw flowrate and the feed flowrates are determined following *IFR*. The number of FO pressure vessels ($N_{V,PF}$) is obtained by dividing the required amount of seawater intake ($Q_{D,intake}$) bound to the RO recovery variations with the initial draw flowrate of the lead element. The vessel cost estimation method was derived from the vessel cost estimation offered by Hydration Technology Innovations, Inc. (Albany, OR, USA). The cost information of a single pressure vessel (\$800) was offered by the PAFO pilot system manufacturer (Cheonha Industries, Gwangju, Korea).

Labour and chemical costs of $OPEX_{PAFO}$ were neglected. A conservative assumption was made that 5 years of FO element replacement frequency based on RO element replacement frequency are required [25]. PAFO pump efficiency (η_{pf}) was assumed to be 0.85. The vessel ratio (*VR*) between the PAFO and RO unit processes was assumed to represent the conversion factor from $OPEX_{RO,P\text{-}M}$ to $OPEX_{PAFO,P\text{-}M}$ since parts and material costs are assumed to be dependent on pipelines connected to the pressure vessels. Also, due to lower operating pressure of PAFO compared to RO, the pressure ratios (*PRF* and *PRD*) for both feed and draw sides were assumed to play a major role in determining the $OPEX_{PAFO,P\text{-}M}$. The number of feed and draw pumps (N_{FP} and N_{DP}) is bound to the number of skids (i.e. one feed and one draw pumps for one skid). The calculation of PAFO energy cost (PP_C) was carried out based on the equation for shaft power of a pump given in [15]. Summary of important assumptions and detailed computation procedures for $CAPEX_{PAFO}$ and $OPEX_{PAFO}$ is given in Table S2. Detailed procedures for determining $CAPEX_{PAFO}$ and $OPEX_{PAFO}$ are illustrated in Fig. 3. Target RO recovery, initial feed and draw flowrates ($QF_{,in}$ and $Q_{D,in}$), ΔP_{serial} and serial connection (SE) are the important independent variables that determine the economic feasibility.

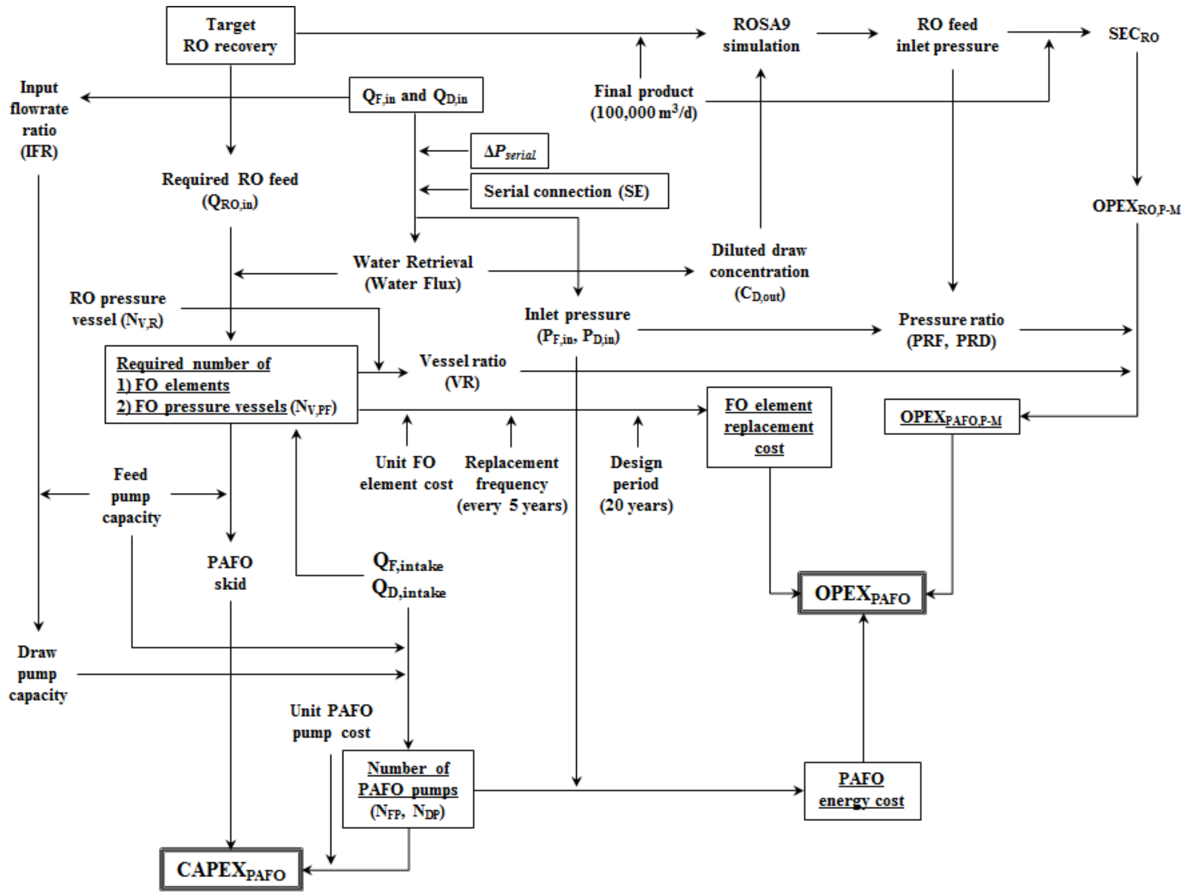

Fig. 3. Procedure for determining $CAPEX_{PAFO}$ and $OPEX_{PAFO}$ (Note: important initial independent variables and the dependent expenditure components are specified with single-lined rectangles)

3. Results and Discussion

3.1. Performance evaluation

3.1.1. Water flux behavior and draw stream dilution

As observed in previous studies [12, 14], impact of $Q_{D,in}$ is greater than that of $Q_{F,in}$ as depicted in Fig. S2 – S4. To better understand the general water flux trend, the data sets (i.e. 3-D planes) shown in Fig. S2 – S4 were averaged with regards to their respective ΔP_{serial} and illustrated in Fig. 4. E1, E2 and E3 denote the first, second and third elements, respectively.

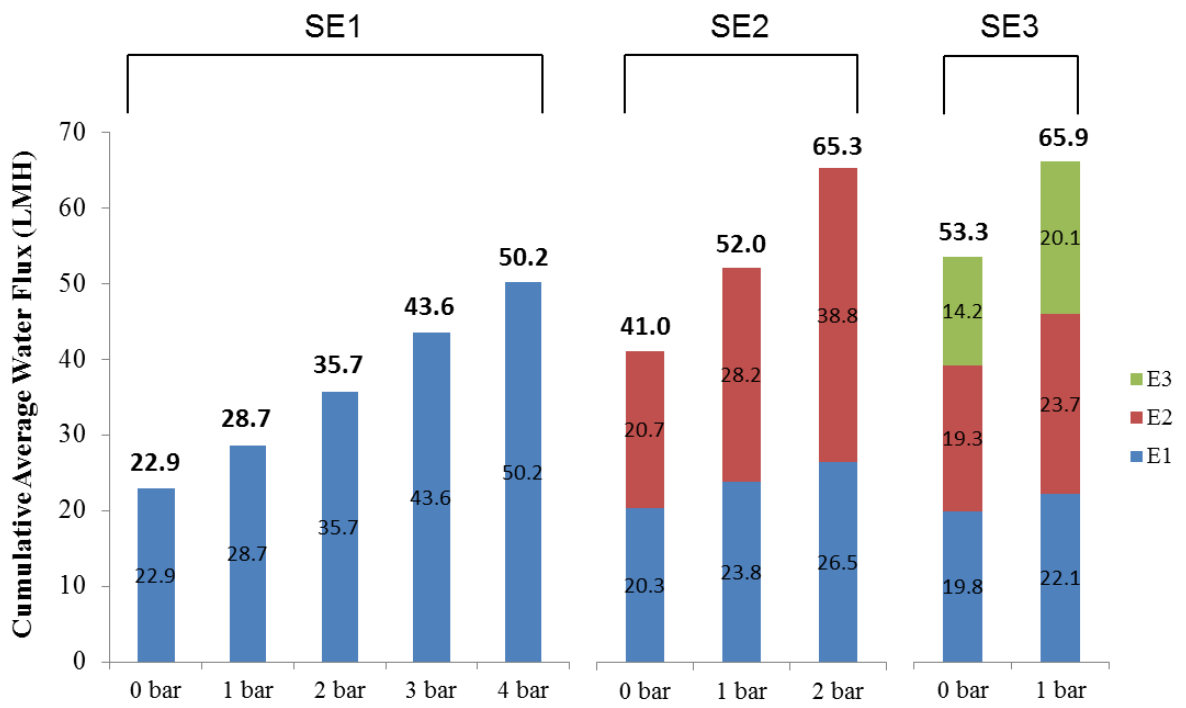

Fig. 4. Cumulative average water flux variations for serial connections with respect to ΔP_{serial}

It is important to note that, for a fixed ΔP_{serial}, water flux of the lead element decreased as the number of serially connected FO elements increased. Similar trend was also observed for the second element. This observation implies that the ability to produce water decreased as the overall channel length increased. At ΔP_{serial} = 0 bar, cumulative average water fluxes of SE2 –

0 bar and SE3 – 0 bar for E1 and E2 (i.e. 41.0 LMH for SE2 and 39.1 LMH for SE3) were comparable. However, cumulative average water fluxes of SE2 – 1 bar and SE3 – 1 bar for E1 and E2 at $\Delta P_{serial} = 1$ bar showed significant difference. Such trend can be clearly observed by comparing the results of E1 as given in Fig. 5. The slopes in Fig. 5 indicate the impacts of hydraulic pressure on water flux improvement by PAFO. Decreasing slopes with increasing SE implies that the effectiveness of pressure difference between the feed and draw channels for water transport deteriorates as the number of serially connected FO elements increases. It can be concluded that the least number of FO elements in series is beneficial for PAFO operation. Nevertheless, the economics of PAFO-RO hybrid is determined by not only the water flux as well as the diluted draw concentration.

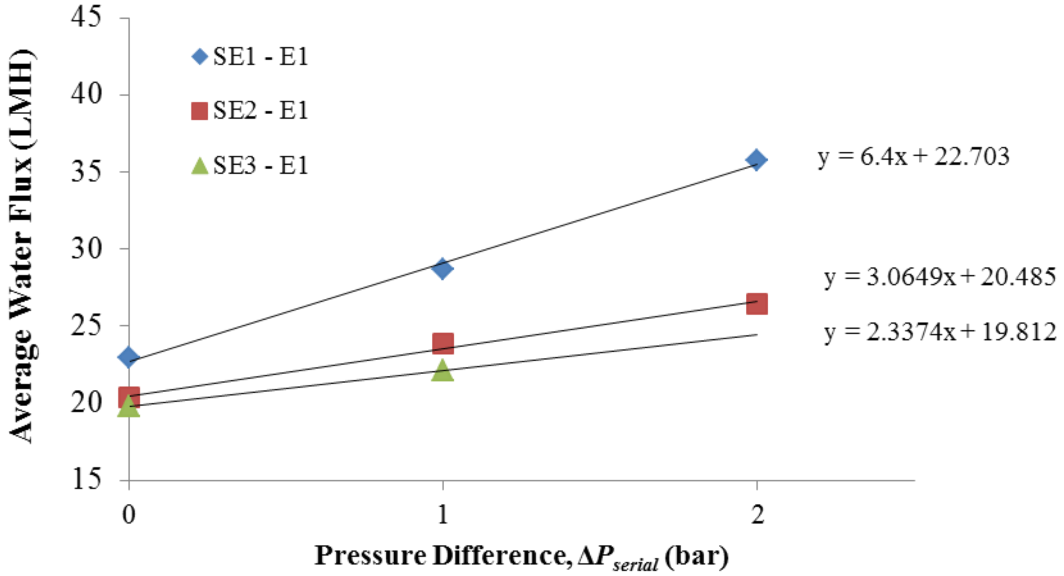

Fig. 5. Impact of serial connection with varying ΔP_{serial}

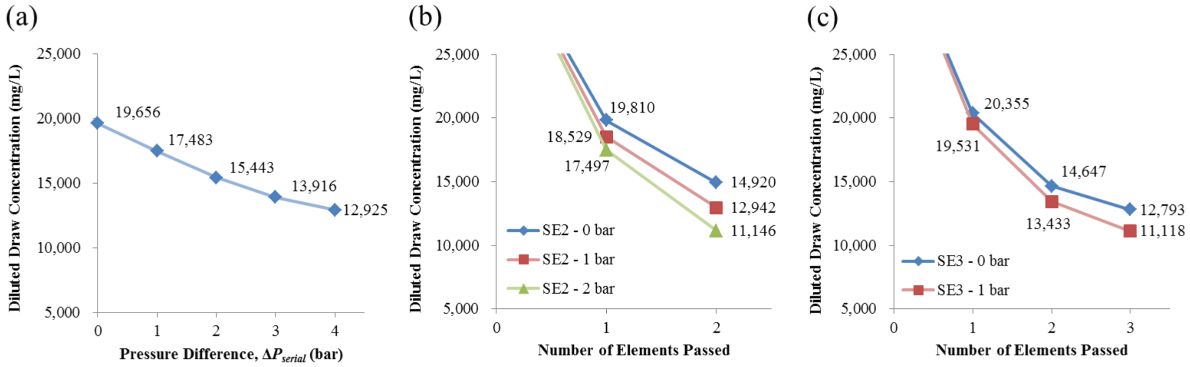

Fig. 6. Diluted draw concentrations for (a) SE1, (b) SE2 and (c) SE3 in accordance with varying ΔP_{serial} (Note: initial draw concentration, $C_{D,in}$ = 35,000 mg/L)

Diluted draw concentration is in close correlation with water flux. The diluted draw concentrations (i.e. Figs. S2b, S3d – S3f and S4c and S4d) were averaged for the specified ΔP_{serial} values and plotted in Fig. 6. In general, for a specific ΔP_{serial} and a designated number of elements passed, diluted draw concentration was higher with higher SE. These trends are in line with the water flux behaviors discussed above. For all SE cases, it can be noticed that the lead element contributed the most to the draw stream dilution. In addition, additional significant concentration reduction was achieved by implementing E2 yet with negligible reduction by E3. This implies that applying SE3 might not be as economically beneficial as it would be for SE1 and SE2 due to the relatively marginal decrease of RO feed concentration. All diluted draw concentrations of the last element were employed as RO feed concentrations ($C_{D,out}$) for economic evaluation.

3.1.2. Hydraulic pressure dependence of FO element performance

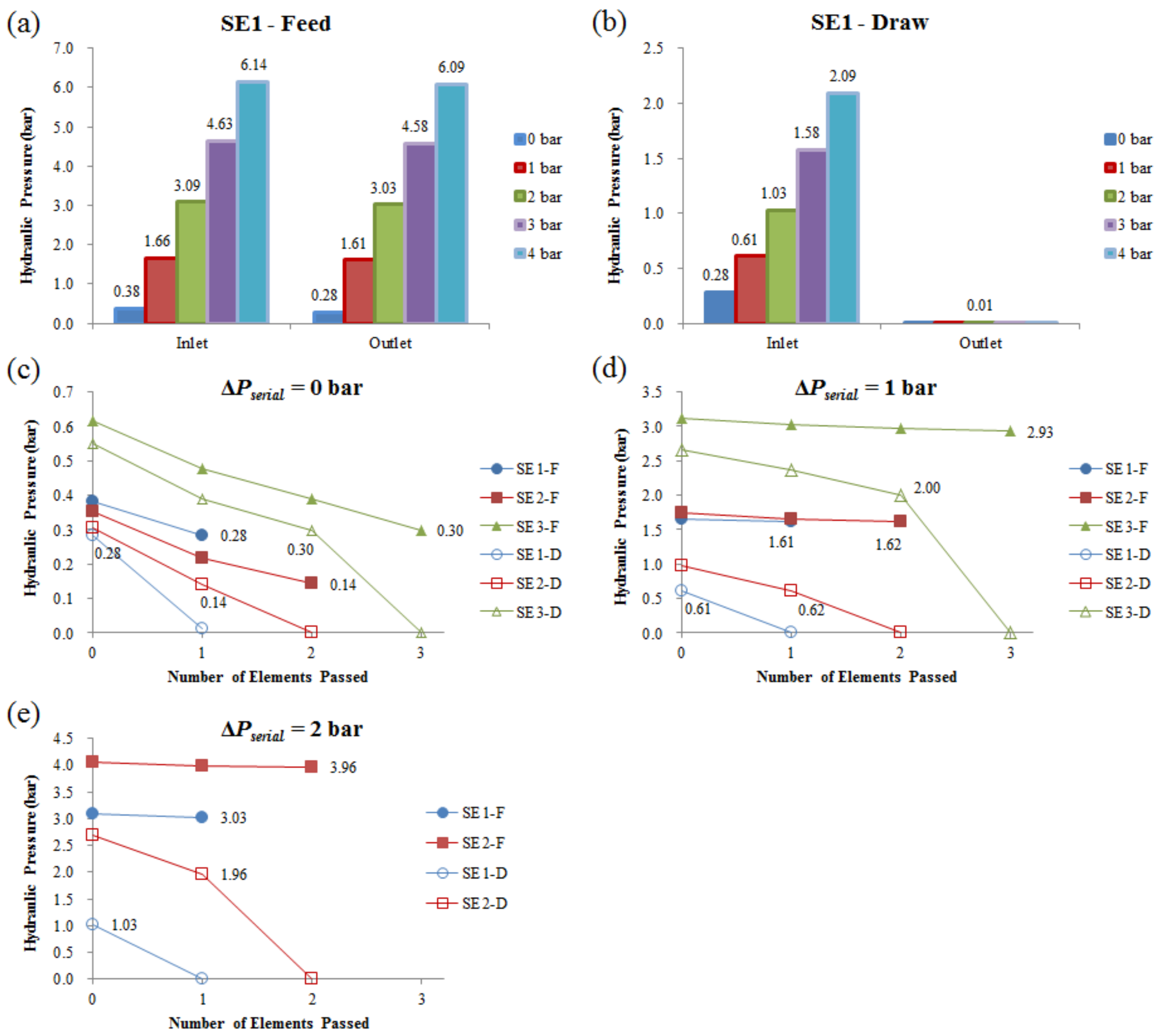

Fig. 7. Hydraulic pressure variations along the serially connected FO elements. (a) feed side and (b) draw side for SE1. Comparison of hydraulic pressure profiles of SE1, SE2 and SE3 for ΔP_{serial} conditions of (c) 0 bar, (d) 1 bar and (e) 2 bar

Based on the previous study [12], increase of the channel length (i.e. serial connection) and the additional hydraulic pressure may negatively affect the economics of PAFO-RO hybrid. Increase of channel length directly leads to the increased structural resistance of the initial water body through the channels. Also, the draw channel contraction induced by additional pressure in the feed side can play a pivotal role in worsening the structural resistance of the draw channel. The coupled effect of these two characteristics is anticipated to generate the major cause of the inlet pressure increase. All pressure values in Fig. S5 are averaged for better display of the trend.

Fig. 7 shows the hydraulic pressure variations along the feed and draw channels in serial connection. All numbered labels in Fig. 7 indicate the average hydraulic pressure conditions that define respective ΔP_{serial} (i.e. $P_{F,out} - P_{D,in}$ of the last element) for SE1, SE2 and SE3 configurations. As depicted in Figs. 7a and 7b, the feed pressure drop (i.e. $P_{F,in} - P_{F,out}$) was low compared to the draw pressure drop (i.e. $P_{D,in} - P_{D,out}$). This can be explained that for the draw channel, water mass transported through the membrane exhibits momentum (i.e. mass x velocity) that is readily transferred to the existing water mass at a specific location of the draw channel. Momentum is a vector quantity for a 3-dimensional space which means the momentum transfer does not necessarily occur only to the draw stream flow direction only. Since draw water body is surrounded by the FO membranes, the momentum transfer can occur into the draw stream flow direction as well as its opposite direction (i.e. toward the draw pump). In the meantime, for water being incompressible body, water mass transport through the membrane enhances inertia per given volume in the draw channel leading to the increase of total head at any given location according to the Navier-Stokes equation in convective form [26]. Starting from the draw inlet location, draw stream velocity increases along the flow path and this leads to the continuous increase of total head toward the draw outlet. However, pressure drop is proportional to velocity squared for a given friction factor and hydraulic radius according to the Darcy-Weisbach equation [27]. This means the pressure drop becomes most severe at the draw outlet.

Based on the assumptions of mass continuity and conservation of mass, pressure variation within the draw channel must be in continuum toward the draw pump in association with the momentum transfer considering the draw outlet pressure and is close to atmospheric pressure (i.e. close to 0 bar in gauge pressure). A severe pressure build-up at the draw inlet consequently arose and resulted in severe draw pressure drop. Unlike the draw channel, the momentum transfer due to water transport is in negative direction for the existing feed water body in the feed channel thereby a minor pressure drop occurs. Nevertheless, this explanation requires further experimental validation which is out of the scope of this study.Similar trends were observed for SE2 and SE3 as illustrated in Figs. 7c, 7d and 7e. The draw pressure drop became significant as ΔP_{serial} increased. The required draw inlet pressures given in Fig. 7 are a critical variable for supplying the target $Q_{D,in}$ into the FO pressure vessel. It is worthwhile to note that the increase of feed inlet pressures with increasing SE is inevitable for appropriate and safe operations of FO elements to maintain ΔP_{serial}. These feed and draw inlet pressures are important for operating factors to be employed for PAFO pump energy cost (PP_C) calculations in the following economic evaluation.

3.2. Economic evaluation

3.2.1. Impact of hydraulic pressure and serial connection

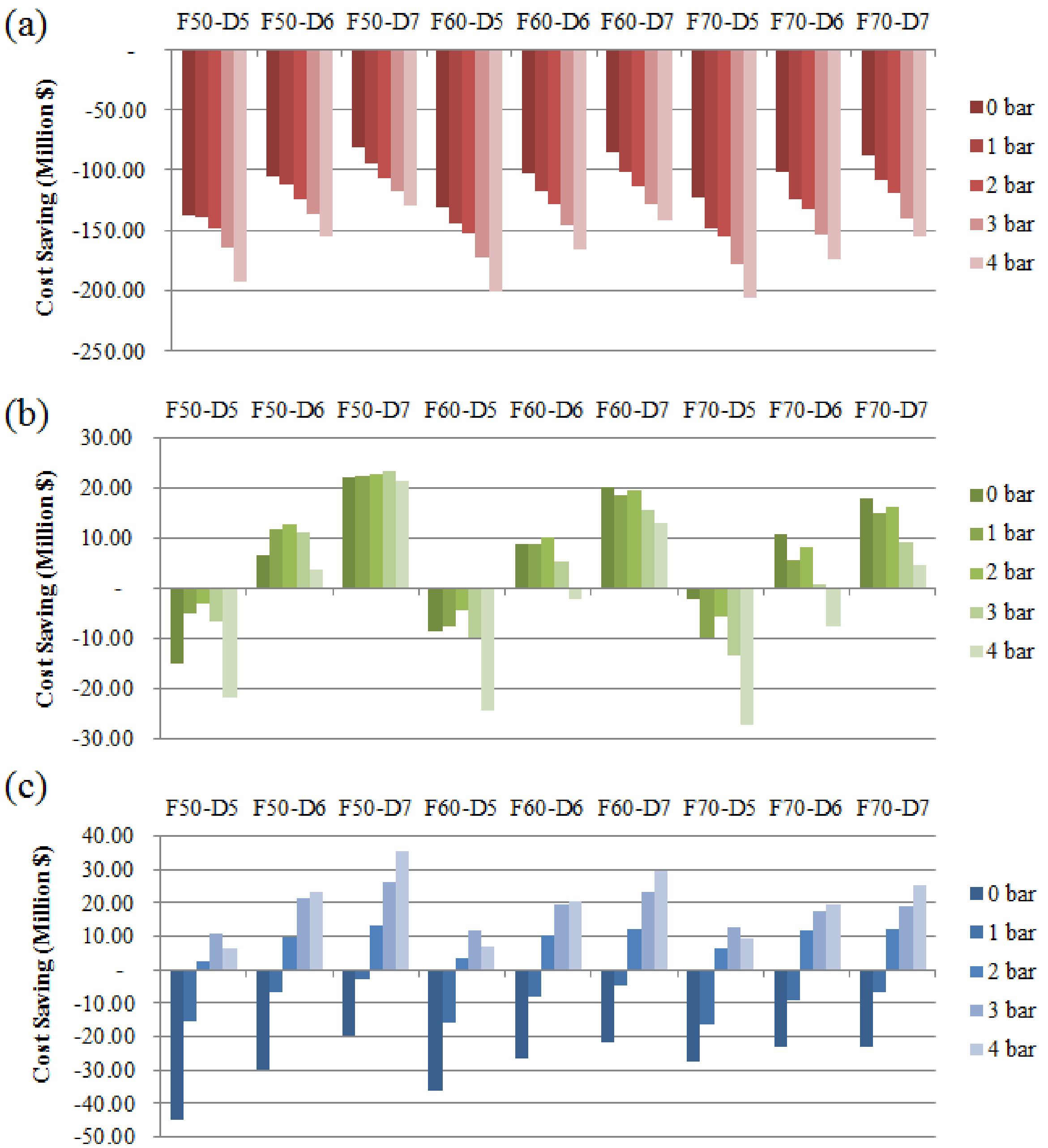

Fig. 8. Variations of cost savings of single element (SE1) scenario for target RO recoveries of (a) 40%, (b) 60% and (c) 80% with varying initial flowrates and ΔP_{serial} when unit FO element cost was $2,000 (Note: F and D denote initial feed and draw flowrates, respectively.)

As shown in Fig. S2 – S4, the impact of initial feed flowrate ($Q_{F,in}$) on water flux is smaller than that of initial draw flowrate ($Q_{D,in}$). Fig. 7 illustrates a perceptible but minor contribution of $Q_{F,in}$ yet a noticeable impact of $Q_{D,in}$. The complexity of the economics of the PAFO-RO hybrid is, in fact, the results of the orderly trends of $OPEX_{RO}$ saving, $CAPEX_{PAFO}$ and $OPEX_{PAFO}$ (Figs. S6 – S14). In the PAFO-RO hybrid system, the major source of cost saving is the reduction of $OPEX_{RO}$ due to improved dilution by additional hydraulic pressure. For a fixed RO recovery and ΔP_{serial}, the increase of $Q_{D,in}$ reduces the required number of FO elements attributed to the increase of water flux (i.e. enhanced water retrieval) which leads to the reduction of $CAPEX_{PAFO}$. This also has a positive contribution to $OPEX_{PAFO}$ since the required number of the PAFO skid and the FO elements decreases. This directly induces the reduction of PAFO pump energy cost with regards to the reduction of the required number of feed and draw pumps as well as the reduction of the number of FO elements to be replaced throughout the specified design period (i.e. DP = 20 years). The increase of target RO recovery accordingly affects the $CAPEX_{PAFO}$ and $OPEX_{PAFO}$ for a positive contribution to the economics of the PAFO-RO hybrid. The increase of $Q_{D,in}$ negatively affects the economics in terms of $OPEX_{RO}$ saving because of the increase of RO feed concentration (i.e. diluted draw concentration) yet to a minor degree since diluted draw concentration is subtly dependent.

Excluding the effect of PAFO energy cost on cost saving, the increase of ΔP_{serial} must reduce the RO energy cost due to enhanced dilution. However, at 40% of the RO target recovery (Fig. 8a), the economic feasibility incrementally deteriorates with the increasing ΔP_{serial}. This indicates that the PAFO energy cost cannot be disregarded at low RO recovery. In fact, the PAFO energy cost is dependent on the required number of feed and draw pumps (i.e. the number of PAFO skid), suggesting that the increase of the target RO recovery efficiently minimizes the negative impact of additional PAFO energy cost on the economics. As can be seen in Figs. 8b and 8c, the cost saving was improved accordingly. However, the increase of

RO recovery from 60% to 80% showed slight reduction of economic feasibility. This is because of the significant increase of SEC_{RO} in the specified range of the RO feed concentrations (i.e. diluted draw concentrations of the last element in Figs. S2b ranging from 12,001 to 20,053 mg/L) at the 80% of recovery as depicted in [14]. This interpretation can be analogously employed for the SE2 and SE3 cases.

Figs. 9 and 10 show the cost savings of SE2 and SE3 scenarios, respectively. The increase of the RO recovery in general showed improved economics as anticipated. For SE2, the diluted draw concentrations at the outlet of the last element varied from 10,166 to 16,017 mg/L, resulting in a narrower concentration variation compared to that of SE1 (i.e. 14,385 – 20053 mg/L for $\Delta P_{serial} = 0 – 2$ bar). The concentration variation for SE3 was observed between 10,202 and 13616 mg/L. The concentration variation was further depressed as opposed to the SE1 and SE2 cases (i.e. 16,722 – 20,053 mg/L for SE1 and 11,782 – 16,017 for SE2 for $\Delta P_{serial} = 0 – 1$ bar). From Figs. 9b and 9c, it can be noticed that the cost savings were improved compared to those of SE1 at higher target RO recoveries. However, in the case of SE3, the cost saving was noticeably deteriorated compared to SE2 primarily due to the inefficient use of FO membrane elements coupled with significant increase of $CAPEX_{PAFO}$ and $OPEX_{PAFO}$. The narrower concentration variations with lower average concentrations compared to SE1 were sufficient enough to yield economic benefits in SE2. However, in SE3, this benefit was further reduced and overwhelmed by the $CAPEX_{PAFO}$ and $OPEX_{PAFO}$ induced by the increase of required number of FO elements. Thus, thoroughly considering the results in Figs. 8 - 10, it can be stated that employing 8040 FO elements in serial connection of three might not be a viable option for PAFO-RO hybrid process when using seawater as draw solution.

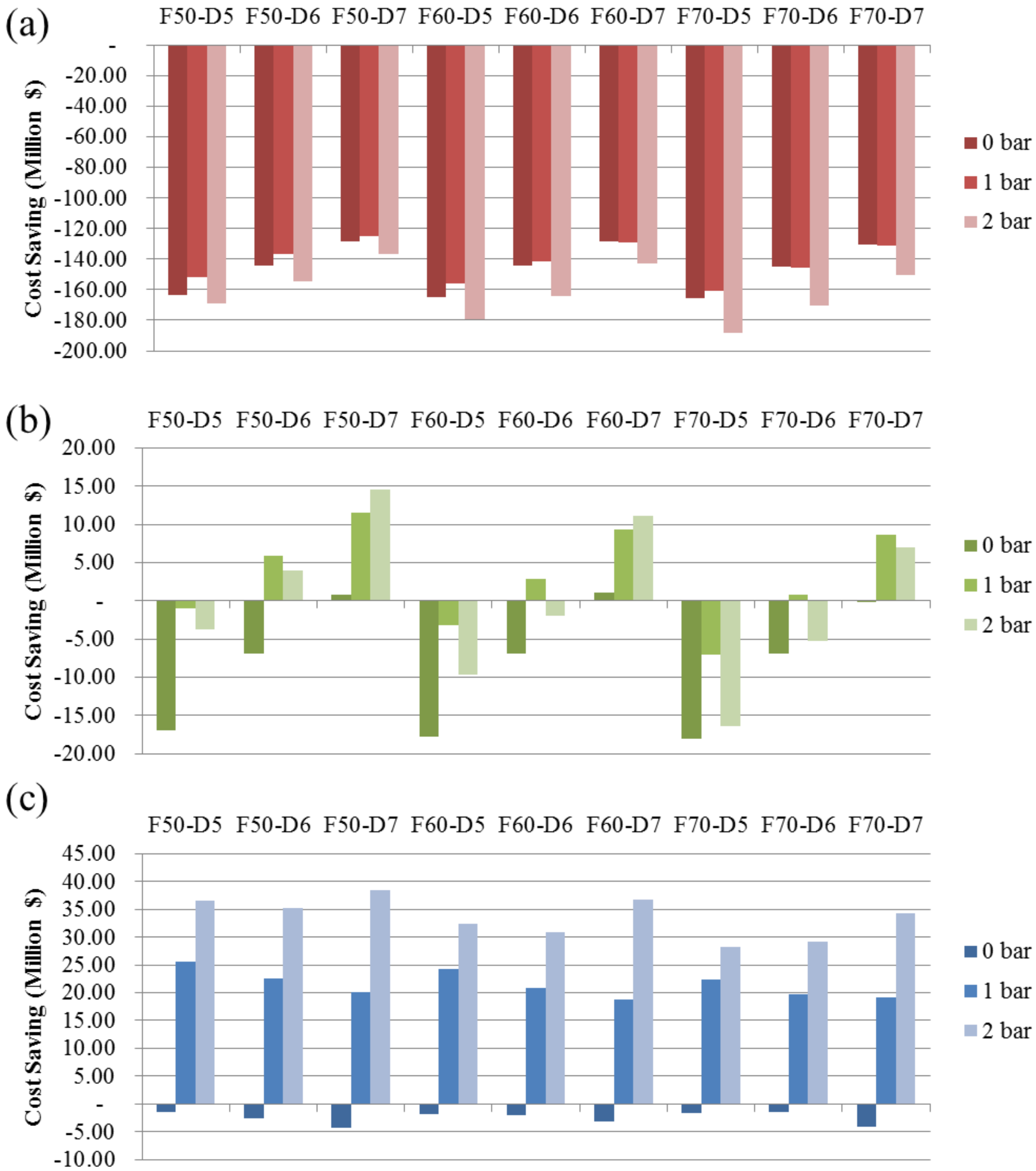

Fig. 9. Variations of cost savings of SE2 scenario bound to identical description in Fig. 8

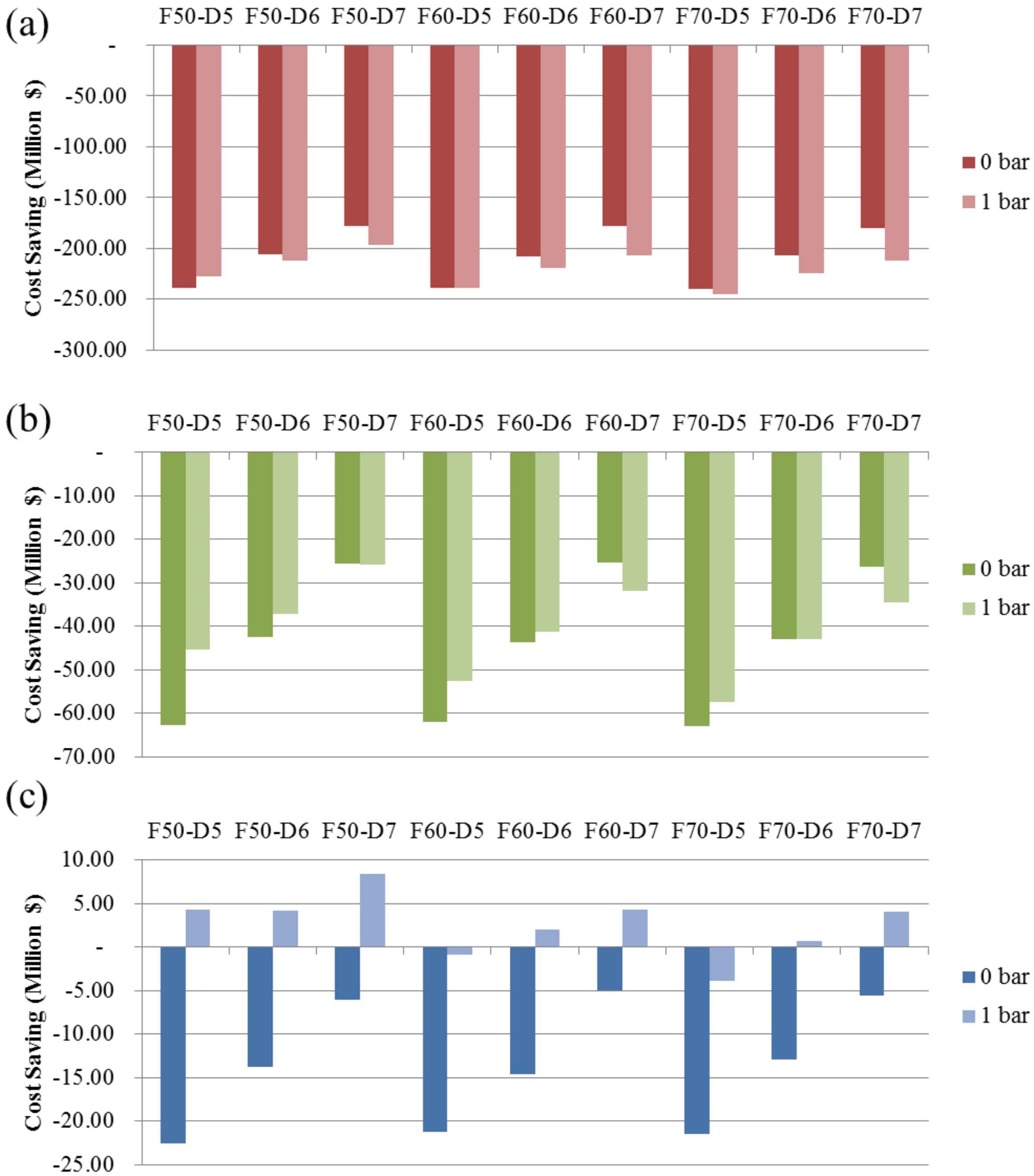

Fig. 10. Variations of cost savings of SE3 scenario bound to identical description in Fig. 8

3.2.2. Determination of optimal operational condition of PAFO for PAFO-RO hybrid

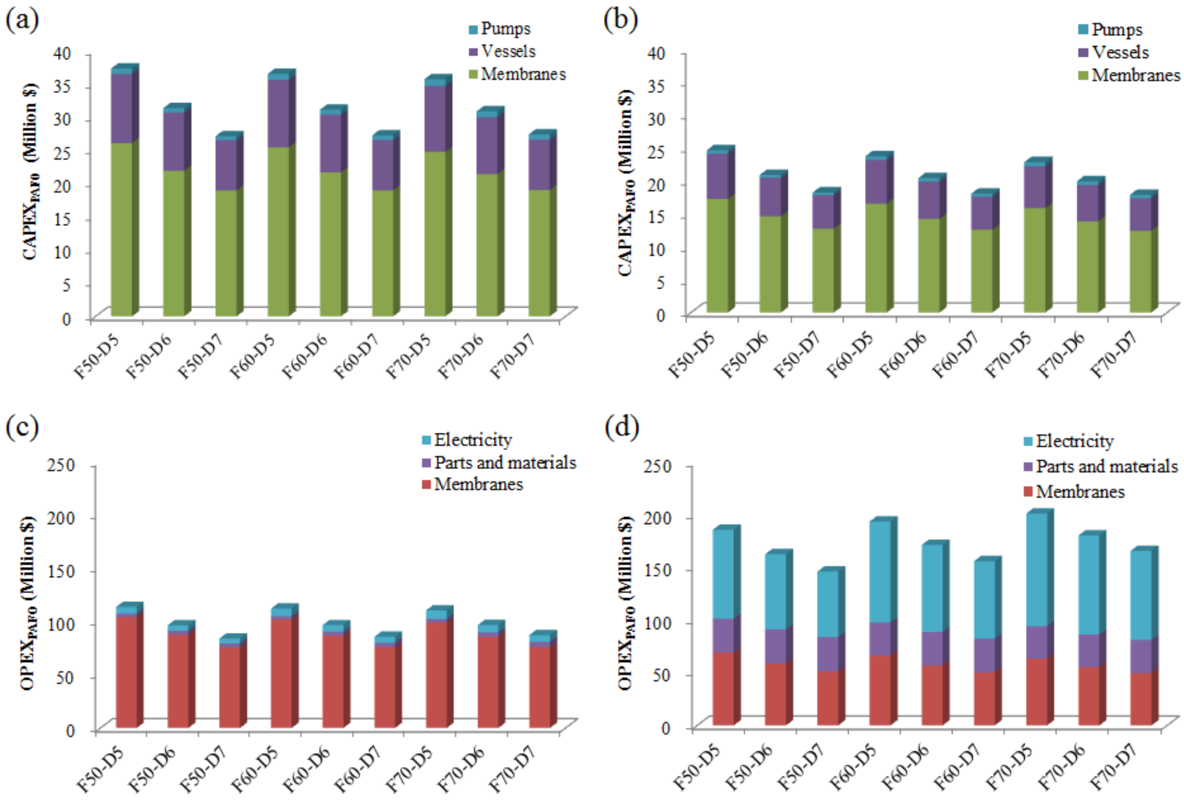

Fig. 11. FO element cost and PAFO energy cost as major components of the economics of PAFO-RO hybrid. Cost saving in $CAPEX_{PAFO}$ by additional pressure ((a) $CAPEX_{PAFO}$ at ΔP_{serial} = 0 bar and (b) $CAPEX_{PAFO}$ at ΔP_{serial} = 4 bar) compensated by the $OPEX_{PAFO}$ due to additional energy cost ((c) $OPEX_{PAFO}$ at ΔP_{serial} = 0 bar and (d) $OPEX_{PAFO}$ at ΔP_{serial} = 4 bar) at 60% target RO recovery for SE1 with $2,000 of unit FO element cost

It is obvious that the economic feasibility of PAFO-RO hybrid will be incrementally improved if FO element cost decreases. However, the decrease of FO element cost alone does not necessarily determine the optimal serial configuration and operational conditions since total cost saving is dependent on the key design operational factors (i.e. target RO recovery, $Q_{D,intake}$ and ΔP_{serial}) as discussed in the previous section. Thoroughly considering the key design factors along with the FO element cost variation, an optimal operational condition can be determined.

As depicted in Fig. 11 as a set of examples for SE1, unit FO element cost is a major component for both $CAPEX_{PAFO}$ and $OPEX_{PAFO}$. Overall economics are primarily dependent on target RO recovery. Total cost savings were averaged in line with the hydraulic pressure variations along the serially connected FO elements (Fig. 7) and plotted as 3-dimensional (3-D) planes in Fig. S15. The corresponding eagle-eye view planes were given in Fig. 12.

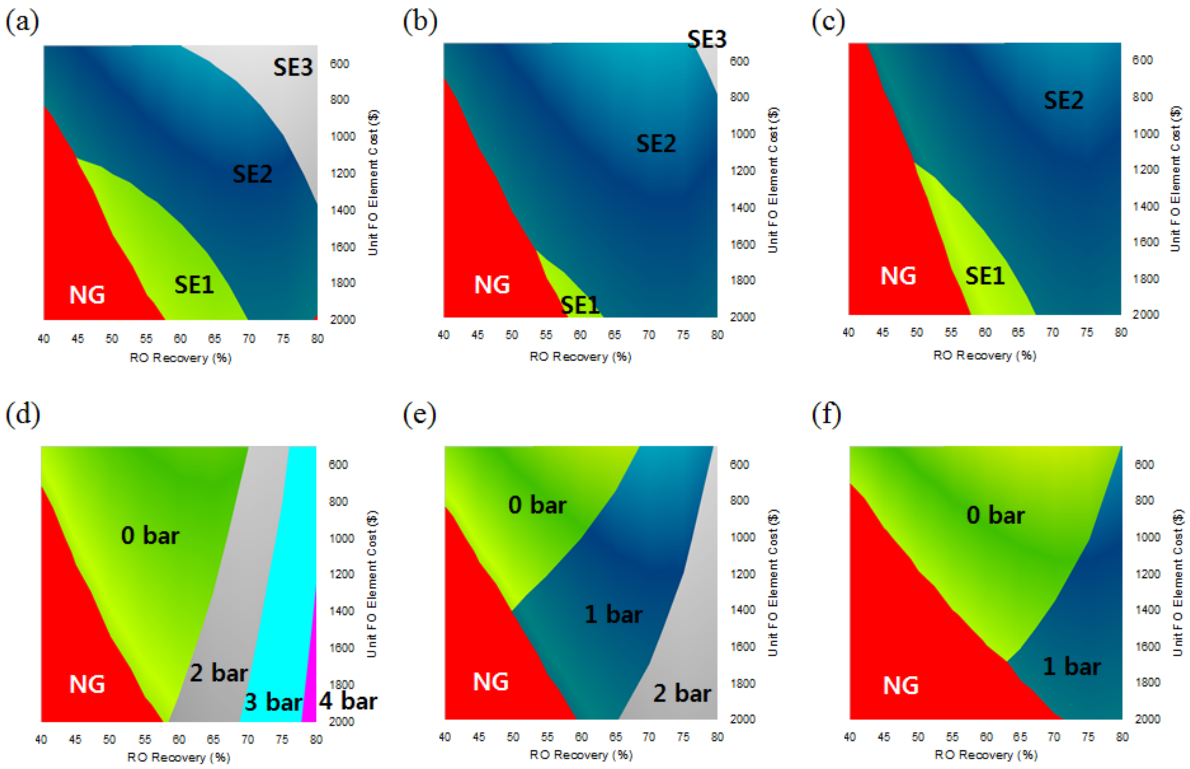

Fig. 12. Determination of optimal operational condition and configuration with respect to target RO recovery and unit FO element cost when ΔP_{serial} is (a) 0 bar, (b) 1 bar, (c) 2 bar or serial connection is (d) SE1, (e) SE2 and (f) SE3 (Note: The red zones specified with the NG (i.e. no-go) notation are economically not feasible for serial configurations and operational conditions.)

In general, the increase of target RO recovery improved the economic feasibility. In relation to hydraulic pressure increase considering the trends shown in Figs. 12a – 12c, the economics of PAFO-RO were deteriorated at lower RO recovery. It is because of the dominance of $OPEX_{PAFO}$

compared to the decrease of $CAPEX_{PAFO}$ and $OPEX_{RO}$ as discussed in the earlier section (i.e. larger required number of FO elements and pressure vessels than higher RO recovery leading to extensive PAFO energy requirement). This dominance of $OPEX_{PAFO}$ can be suppressed by increasing the RO recovery. Also, the decrease of unit FO element cost noticeably reduced the $CAPEX_{PAFO}$ and $OPEX_{PAFO}$ resulting in the observed trends. In practical perspective, unit FO element cost is typically fixed and thus the implementation of PAFO unit process to the existing 2-stage RO process can be optimized by controlling the target RO recovery and selecting the best serial configuration. Within the operating range of $Q_{F,in}$ and $Q_{D,in}$ tested in this study, SE2 showed the most significant plausibility throughout. The SE3 scenario can only be beneficial when the element cost is significantly reduced. According to the FO element manufacturer, the unit FO element cost was $2,000 thus the SE3 option should be discarded at this stage. Considering the wider area for SE1 in Fig. 12c, further increase of hydraulic pressure can enable the SE1 option to become incrementally beneficial compared to the SE2 case in the target RO recovery range of approximately 60 – 67%. However, Figs. 12a – 12c are only applicable to respective serial configuration scenario. At this point, a thorough consideration on both ΔP_{serial} and SE variations is necessary.

Overlapping the top and the bottom figures can give a clearer idea on what serial configuration is beneficial at what specific operating RO recovery and hydraulic pressure. By overlapping the specified ranges representing serial connection scenarios in Fig. 12a with the respectively corresponding green areas in Figs. 12d – 12f (i.e. ΔP_{serial} = 0 bar), it can be noticed that FO-RO hybrid is not beneficial unless the membrane cost is significantly reduced from the current unit FO element cost. Similarly overlapping the specified areas in Fig. 12b with the respective blue areas in the bottom figures (i.e. ΔP_{serial} = 1 bar), it can be clearly seen that the SE1 and SE3 scenarios are not the optimal configurations and the SE2 scenario is the only available option. By applying the identical assessment on Fig. 12c (i.e. ΔP_{serial} = 2 bar), a small optimal area for SE1 within the RO recovery of approximately 60 – 67% and a larger area for SE2 in higher RO recoveries of approximately 67 – 80%. In summary, the FO-RO hybrid option can only be beneficial when significant unit FO element cost reduction is possible whereas the SE2 scenario is a viable option for higher range of RO recovery. In addition, the serial connection of more than 8040 FO elements is not an economically feasible option for FO-RO hybrid due to the overwhelming CAPEX and OPEX of FO over energy cost saving in RO. Same for PAFO-RO due to exponential increase of inlet hydraulic pressure leading to escalating $OPEX_{PAFO}$ of negative dominance in economic feasibility over $OPEX_{RO}$ saving. This graphical evaluation method can be a practically valid tool to determine the optimal serial configuration and operating condition depending on the membrane cost.

3.2.3. Strategy for improving economic feasibility

In this economic evaluation, a limited number of $CAPEX_{PAFO}$ (i.e. FO element, PAFO pumps and pressure vessels) and $OPEX_{PAFO}$ (i.e. PAFO electricity cost, PAFO parts and material and FO membrane replacement) components were assessed. Considering both the capital expenditure for civil engineering in RO (i.e. 17.31% of $CAPEX_{RO}$ from Fig. S1b) and the larger footprint required for PAFO trains, the costs of civil engineering for employing PAFO to the existing 2-stage RO plant surely decrease the economic feasibility. The larger footprint indirectly indicate that other $CAPEX_{PAFO}$ components such as equipment and materials, piping/high alloy and installation and services can overwhelm the total cost savings estimated in this evaluation. In terms of $OPEX_{PAFO}$, labour and chemical costs are likely to further worsen the economics. Considering these aspects, it can be arguably stated that adopting PAFO to an existing RO plant might not be an economically feasible consideration.

Nevertheless, there are other potential sources that can improve the feasibility of PAFO-RO hybrid process if the hybrid process is newly commissioned as a whole. In the current economic evaluation, $Q_{D,intake}$ was reduced by approximately 40 – 70% depending on operating conditions compared to stand-alone 2-stage RO. This directly leads to an analogy that the corresponding $CAPEX_{RO}$ components such as equipment and materials (22.90%), civil engineering (17.31%), piping/high alloy (14.25%), pretreatment (8.65%) and intake/outfall (7.13%) in Fig. S1b, with a total sum of 70.24% ($90.61 million) of $CAPEX_{RO}$, can be the additional sources for improving the economics of PAFO-RO. In addition, major portion of the RO chemical cost (18.8% of $OPEX_{RO}$, $110.24 million from Fig. S1c) is dedicated to the pretreatment step [28]. Due to the reduced pretreatment capacity, certain degree of electricity cost for other installations can be accordingly reduced. As such, significant reduction of seawater intake itself can improve the overall plant economics. Elongation of design period (*DP*) can also positively affect the economics in the long-term due to accumulating RO energy cost saving. In addition, the likelihood of potential energy crisis breakout in regards to the rapid depletion of fossil fuel-based energy sources [29] can necessitate the desalination means such FO-RO or PAFO-RO hybrid processes of lower energy dependency.

4. Conclusions

The economics of PAFO-RO hybrid process are challenging due to the uncertainties of largely unknown behaviors of $CAPEX_{PAFO}$ and $OPEX_{PAFO}$ components. However, a certain degree of validation was made by conducting an economic assessment based on pilot-scale PAFO experiments using serially connected FO elements on the case in which PAFO is employed as a pretreatment step to an existing 2-stage RO desalination plant. It was also found that the serial connection of FO elements is strongly dependent on the hydraulic pressure and the increase of the operating hydraulic pressure necessitated exponential increase of inlet hydraulic pressures for maintaining the desired initial feed and draw flowrates. Draw dilution was efficient up to serial connection of two FO elements (SE1), yet this effect was significantly deteriorated during testing three elements (SE3). Based on these results, the economic evaluation reached to a conclusion that the SE2 scenario at target RO recoveries higher than 67% is the most economically feasible option within the PAFO-RO hybrid system. Along with the impact of RO recovery on the economics, the unit FO element cost significantly affected the feasibility in terms of determining optimal serial configuration and operating hydraulic pressure conditions. The graphical evaluation method suggested in this work successfully validated the economic feasibility of PAFO-RO hybrid when a limited number of important $CAPEX_{PAFO}$ and $OPEX_{PAFO}$ components are considered in accordance with the pilot-scale experimental results.

Nevertheless, the plausibility of implementing PAFO to an existing RO plant still remained uncertain because of additional $CAPEX_{PAFO}$ components for the construction of the PAFO unit process. This plausibility can be improved by commissioning a PAFO-RO hybrid desalination plant because of the reduction of seawater intake which can lead to a significant reduction of both $CAPEX_{RO}$ and $OPEX_{RO}$. In addition, considering the strict dependence of PAFO-RO economics on unit FO element cost, element manufacturing cost should be reduced when selecting the raw materials to improve the economic feasibility of the hybrid process.

Acknowledgements

This research was supported by a grant (code 18IFIP-B088091-05) from the Industrial Facilities & Infrastructure Research Program funded by Ministry of Land, Infrastructure and Transport of the Korean government.

References

[1] J.R. McCutcheon, R.L. McGinnis, M. Elimelech, A novel ammonia—carbon dioxide forward (direct) osmosis desalination process, Desalination, 174 (2005) 1-11.

[2] D.L. Shaffer, J.R. Werber, H. Jaramillo, S. Lin, M. Elimelech, Forward osmosis: Where are we now?, Desalination, 356 (2015) 271-284.

[3] J.R. McCutcheon, R.L. McGinnis, M. Elimelech, Desalination by ammonia–carbon dioxide forward osmosis: Influence of draw and feed solution concentrations on process performance, Journal of Membrane Science, 278 (2006) 114-123.

[4] J.R. McCutcheon, M. Elimelech, Influence of concentrative and dilutive internal concentration polarization on flux behavior in forward osmosis, Journal of Membrane Science, 284 (2006) 237-247.

[5] D.L. Shaffer, N.Y. Yip, J. Gilron, M. Elimelech, Seawater desalination for agriculture by integrated forward and reverse osmosis: Improved product water quality for potentially less energy, Journal of Membrane Science, 415–416 (2012) 1-8.

[6] DesalData.com, in.

[7] G. Blandin, A.R.D. Verliefde, C.Y. Tang, A.E. Childress, P. Le-Clech, Validation of assisted forward osmosis (AFO) process: Impact of hydraulic pressure, Journal of Membrane Science, 447 (2013) 1-11.

[8] G. Blandin, A. Verliefde, P. Le-Clech, Pressure-assisted osmosis (PAO)–RO hybrid: impact of hydraulic pressure on fouling and economics, Desalination and Water Treatment, 55 (2015) 3160-3161.

[9] Y. Oh, S. Lee, M. Elimelech, S. Lee, S. Hong, Effect of hydraulic pressure and membrane orientation on water flux and reverse solute flux in pressure assisted osmosis, Journal of Membrane Science, 465 (2014) 159-166.

[10] T. Yun, Y.-J. Kim, S. Lee, S. Hong, G.I. Kim, Flux behavior and membrane fouling in

pressure-assisted forward osmosis, Desalination and Water Treatment, 52 (2013) 564-569.
[11] R. Valladares Linares, Z. Li, V. Yangali-Quintanilla, N. Ghaffour, G. Amy, T. Leiknes, J.S. Vrouwenvelder, Life cycle cost of a hybrid forward osmosis - low pressure reverse osmosis system for seawater desalination and wastewater recovery, Water Res, 88 (2016) 225-234.
[12] S.-J. Im, G.-W. Go, S.-H. Lee, G.-H. Park, A. Jang, Performance evaluation of two-stage spiral wound forward osmosis elements at various operation conditions, Desalination and Water Treatment, 57 (2016) 1-12.
[13] Y.C. Kim, S.J. Park, Experimental study of a 4040 spiral-wound forward-osmosis membrane module, Environ Sci Technol, 45 (2011) 7737-7745.
[14] S. Kook, J. Kim, S.-J. Kim, J. Lee, D. Han, S. Phuntsho, W.-G. Shim, M. Hwang, H.K. Shon, I.S. Kim, Effect of initial feed and draw flowrates on performance of an 8040 spiral-wound forward osmosis membrane element, Desalination and Water Treatment, 72 (2017) 1-12.
[15] G. Blandin, A.R.D. Verliefde, C.Y. Tang, P. Le-Clech, Opportunities to reach economic sustainability in forward osmosis–reverse osmosis hybrids for seawater desalination, Desalination, 363 (2015) 26-36.
[16] J.E. Kim, S. Phuntsho, F. Lotfi, H.K. Shon, Investigation of pilot-scale 8040 FO membrane module under different operating conditions for brackish water desalination, Desalination and Water Treatment, 53 (2014) 2782-2791.
[17] B. Lian, G. Blandin, G. Leslie, P. Le-Clech, Impact of module design in forward osmosis and pressure assisted osmosis: An experimental and numerical study, Desalination, 426 (2018) 108-117.
[18] S.-J. Kim, S. Kook, B.E. O'Rourke, J. Lee, M. Hwang, Y. Kobayashi, R. Suzuki, I.S. Kim, Characterization of pore size distribution (PSD) in cellulose triacetate (CTA) and

polyamide (PA) thin active layers by positron annihilation lifetime spectroscopy (PALS) and fractional rejection (FR) method, Journal of Membrane Science, 527 (2017) 143-151.

[19] J. Lee, S. Kook, C. Lee, I.S. Kim, Effect of intermittent pressure-assisted forward osmosis (I-PAFO) on organic fouling, Desalination, 419 (2017) 60-69.

[20] S. Kook, C.D. Swetha, J. Lee, C. Lee, T. Fane, I.S. Kim, Forward Osmosis Membranes under Null-Pressure Condition: Do Hydraulic and Osmotic Pressures Have Identical Nature?, Environ Sci Technol, 52 (2018) 3556-3566.

[21] <GWI IDA Yearbook 2017- 2018.pdf>.

[22] B. Qi, Y. Wang, Z. Wang, Y. Zhang, S. Xu, S. Wang, Theoretical Investigation on Internal Leakage and Its Effect on the Efficiency of Fluid Switcher-Energy Recovery Device for Reverse Osmosis Desalting Plant, Chinese Journal of Chemical Engineering, 21 (2013) 1216-1223.

[23] A. Jiang, L.T. Biegler, J. Wang, W. Cheng, Q. Ding, S. Jiangzhou, Optimal operations for large-scale seawater reverse osmosis networks, Journal of Membrane Science, 476 (2015) 508-524.

[24] D. Scott, Advanced Materials for Water Handling: Composites and Thermoplastics, Elsevier Science Ltd., Kidlington, United Kingdom, 2000.

[25] R. Baker, Membrane Technology and Applications, 2 ed., Wiley, West Sussex, England, 2004.

[26] G. Batchelor, An Introduction to Fluid Dynamics, Cambridge Mathematical Library ed., Cambridge University Press, Cambridge, United Kingdom, 2000.

[27] G. Brown, The History of the Darcy-Weisbach Equation for Pipe Flow Resistance, 2002.

[28] <section5costs.pdf>.

[29] World Bank Commodity Prica Data, Crude Oil Price Forecast: Long Term 2016 to 2025 | Data and Charts, in, 2016.

Figure captions

Fig. 1. Structural characteristics of a spiral-wound FO element and the spacer configurations of the membrane leaves of CSM FO-8040

Fig. 2. Process flow diagram of the PAFO pilot system

Fig. 3. Procedure for determining $CAPEX_{PAFO}$ and $OPEX_{PAFO}$ (Note: important initial independent variables and the dependent expenditure components are specified with single-lined rectangles)

Fig. 4. Cumulative average water flux variations for serial connections with respect to ΔP_{serial}

Fig. 5. Impact of serial connection with varying ΔP_{serial}

Fig. 6. Diluted draw concentrations for (a) SE1, (b) SE2 and (c) SE3 in accordance with varying ΔP_{serial} (Note: initial draw concentration, $C_{D,in}$ = 35,000 mg/L)

Fig. 7. Hydraulic pressure variations along the serially connected FO elements. (a) feed side and (b) draw side for SE1. Comparison of hydraulic pressure profiles of SE1, SE2 and SE3 for ΔP_{serial} conditions of (c) 0 bar, (d) 1 bar and (e) 2 bar

Fig. 8. Variations of cost savings of single element (SE1) scenario for target RO recoveries of (a) 40%, (b) 60% and (c) 80% with varying initial flowrates and ΔP_{serial} when unit FO element cost was $2,000 (Note: F and D denote initial feed and draw flowrates, respectively.)

Fig. 9. Variations of cost savings of SE2 scenario bound to identical description in Fig. 8

Fig. 10. Variations of cost savings of SE3 scenario bound to identical description in Fig. 8

Fig. 11. FO element cost and PAFO energy cost as major components of the economics of PAFO-RO hybrid. Cost saving in $CAPEX_{PAFO}$ by additional pressure ((a) $CAPEX_{PAFO}$ at ΔP_{serial} = 0 bar and (b) $CAPEX_{PAFO}$ at ΔP_{serial} = 4 bar) compensated by the $OPEX_{PAFO}$ due to additional energy cost ((c) $OPEX_{PAFO}$ at ΔP_{serial} = 0 bar and (d) $OPEX_{PAFO}$ at ΔP_{serial} = 4 bar) at 60% target RO recovery for SE1 with $2,000 of unit FO element cost

Fig. 12. Determination of optimal operational condition and configuration with respect to target RO recovery and unit FO element cost when ΔP_{serial} is (a) 0 bar, (b) 1 bar, (c) 2 bar or serial connection is (d) SE1, (e) SE2 and (f) SE3 (Note: The red zones specified with the NG (i.e. no-go) notation are economically not feasible serial configurations and operational conditions.)

Figures

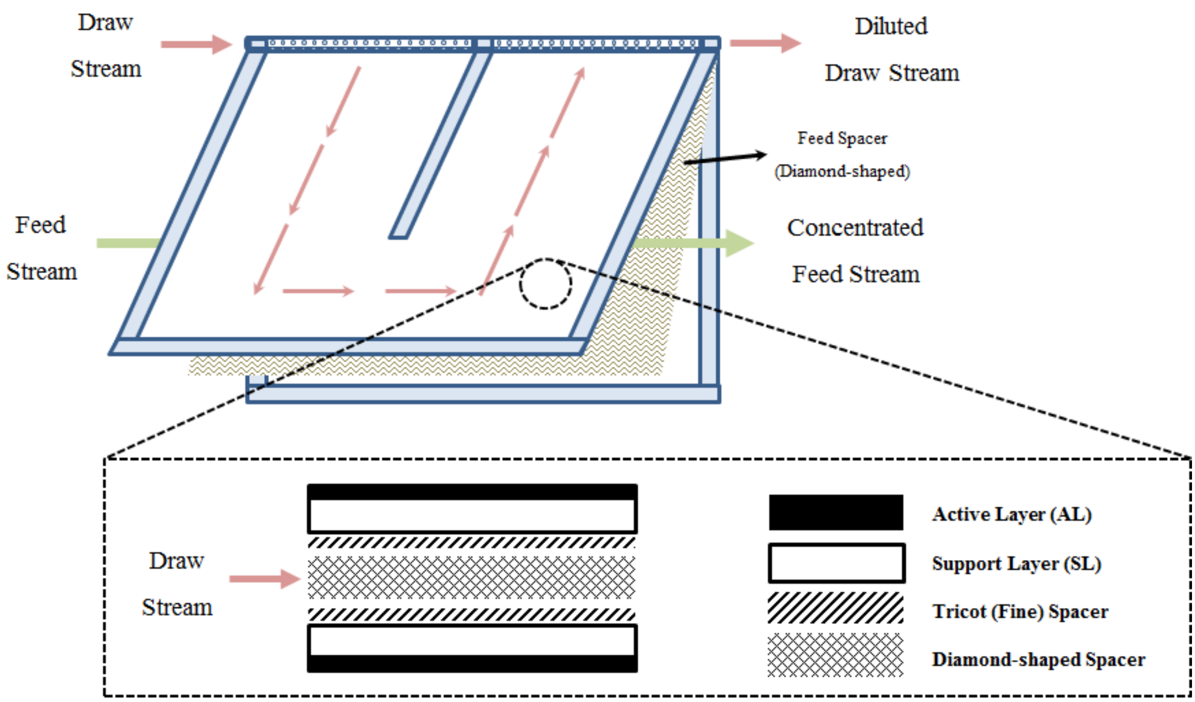

Fig. 1.

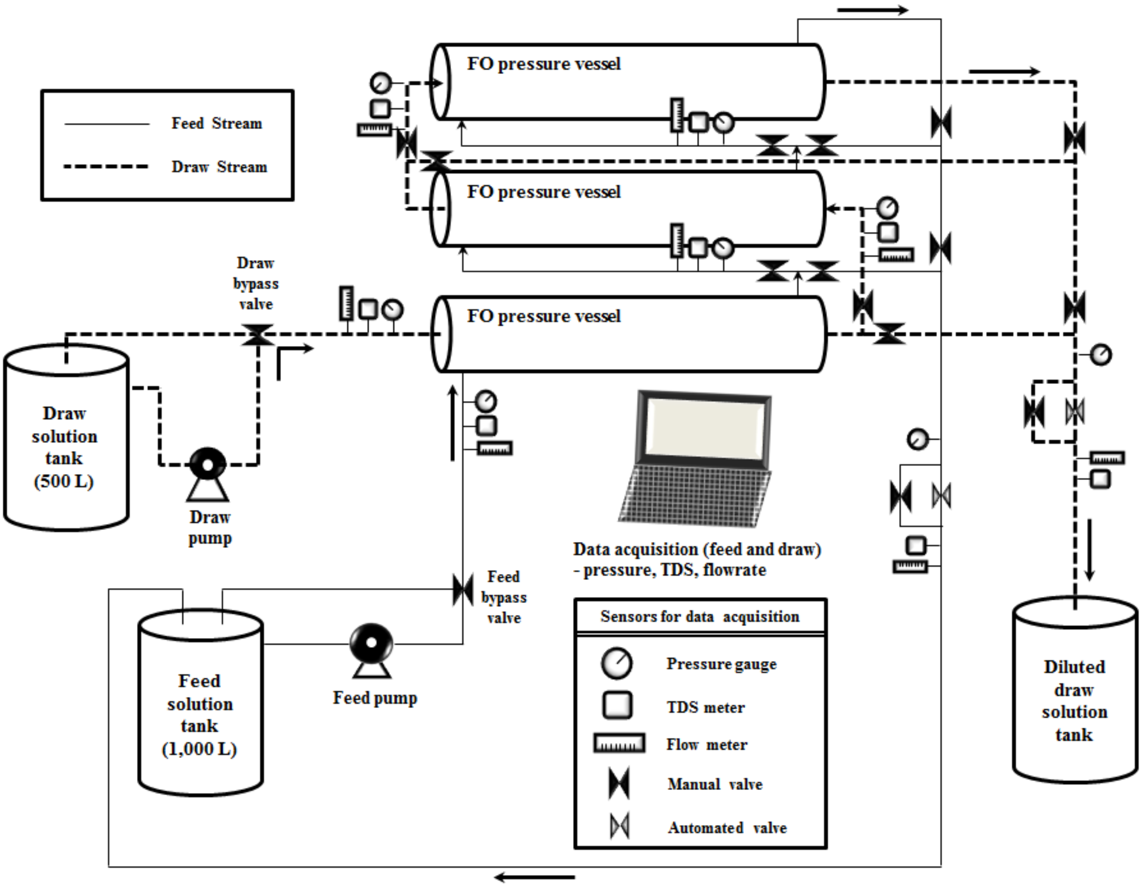
Feed Stream
Draw Stream
FO pressure vessel
FO pressure vessel
FO pressure vessel
Draw bypass valve
Draw solution tank (500 L)
Draw pump
Data acquisition (feed and draw) - pressure, TDS, flowrate
Feed bypass valve
Feed solution tank (1,000 L)
Feed pump
Sensors for data acquisition
Pressure gauge
TDS meter
Flow meter
Manual valve
Automated valve
Diluted draw solution tank

1

2 **Fig. 2.**

3

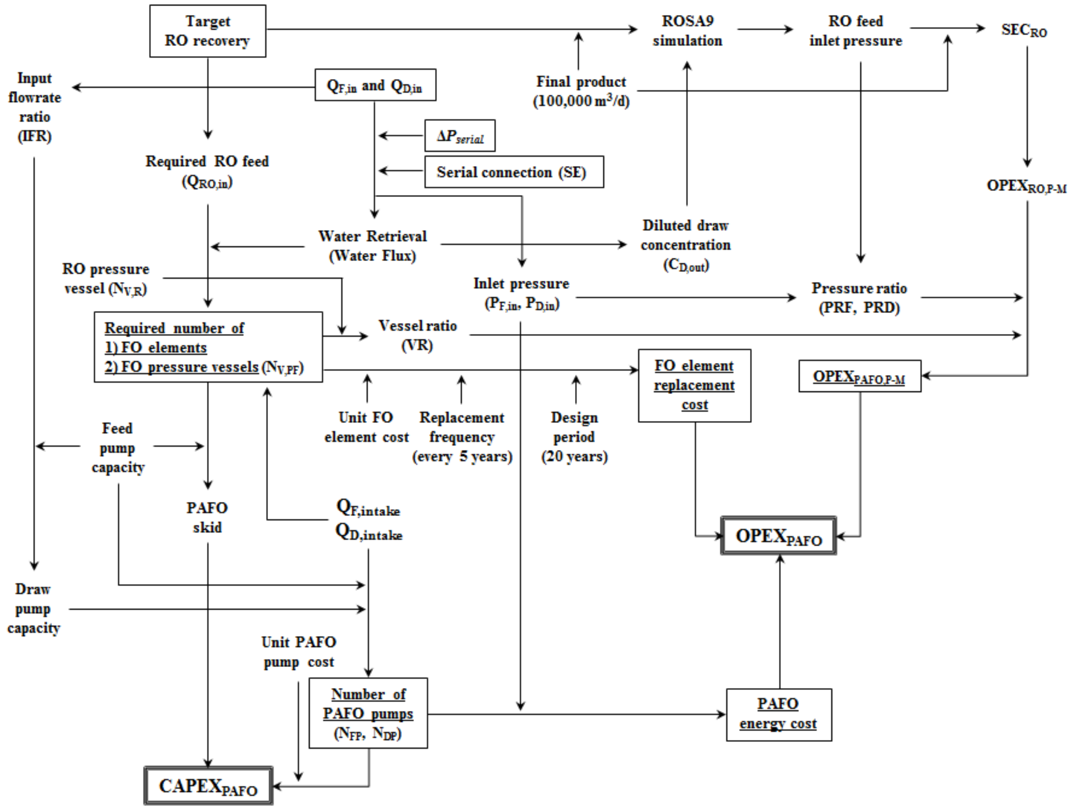
Target RO recovery
ROSA9 simulation
RO feed inlet pressure
SEC_{RO}
Input flowrate ratio (IFR)
$Q_{F,in}$ and $Q_{D,in}$
Final product (100,000 m³/d)
ΔP_{serial}
Serial connection (SE)
Required RO feed ($Q_{RO,in}$)
$OPEX_{RO,P-M}$
Water Retrieval (Water Flux)
Diluted draw concentration ($C_{D,out}$)
RO pressure vessel ($N_{V,R}$)
Inlet pressure ($P_{F,in}$, $P_{D,in}$)
Pressure ratio (PRF, PRD)
Required number of 1) FO elements 2) FO pressure vessels ($N_{V,PF}$)
Vessel ratio (VR)
FO element replacement cost
$OPEX_{PAFO,P-M}$
Unit FO element cost
Replacement frequency (every 5 years)
Design period (20 years)
Feed pump capacity
PAFO skid
$Q_{F,intake}$
$Q_{D,intake}$
$OPEX_{PAFO}$
Draw pump capacity
Unit PAFO pump cost
Number of PAFO pumps (N_{FP}, N_{DP})
PAFO energy cost
$CAPEX_{PAFO}$

Fig. 3.

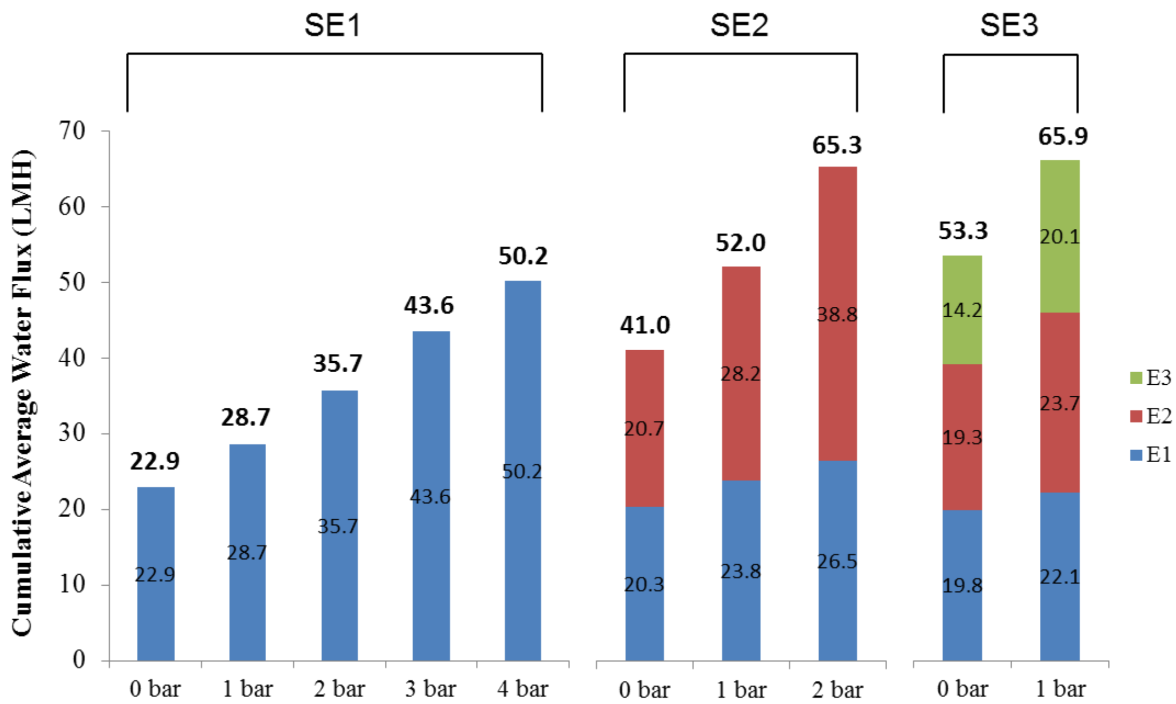
SE1
SE2
SE3
Cumulative Average Water Flux (LMH)
70
60
50
40
30
20
10
0
22.9
28.7
35.7
43.6
50.2
41.0
52.0
65.3
53.3
65.9
20.3
20.7
23.8
28.2
26.5
38.8
19.8
19.3
14.2
22.1
23.7
20.1
E3
E2
E1
0 bar
1 bar
2 bar
3 bar
4 bar
0 bar
1 bar
2 bar
0 bar
1 bar

Fig. 4.

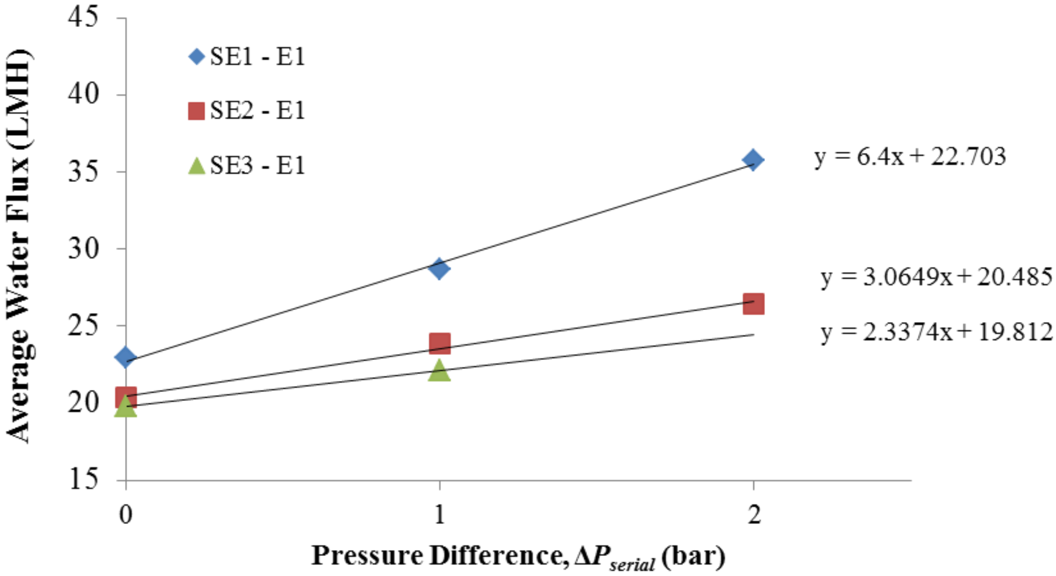

Average Water Flux (LMH)
45
40
35
30
25
20
15
SE1 - E1
SE2 - E1
SE3 - E1
y = 6.4x + 22.703
y = 3.0649x + 20.485
y = 2.3374x + 19.812
0
1
2
Pressure Difference, ΔP serial (bar)

Fig. 5.

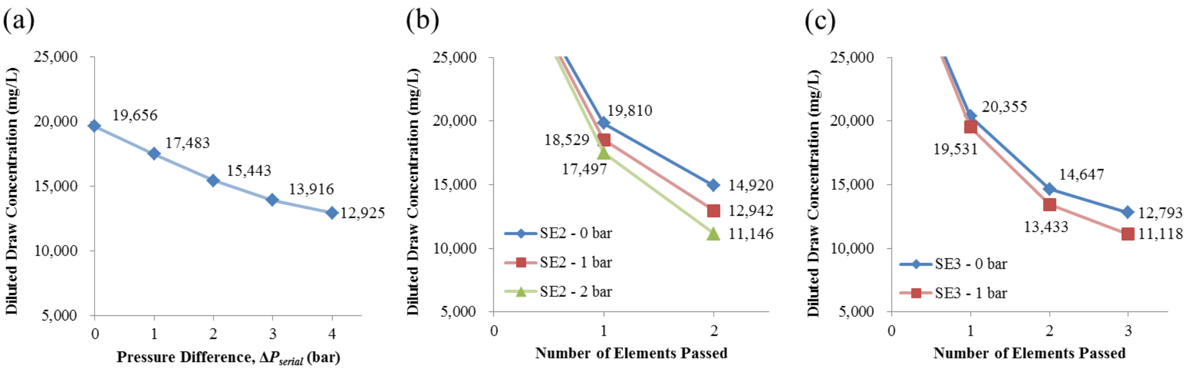

(a)
(b)
(c)
Diluted Draw Concentration (mg/L)
25,000
20,000
15,000
10,000
5,000
19,656
17,483
15,443
13,916
12,925
Pressure Difference, ΔP serial (bar)
19,810
18,529
17,497
14,920
12,942
11,146
SE2 - 0 bar
SE2 - 1 bar
SE2 - 2 bar
Number of Elements Passed
20,355
19,531
14,647
13,433
12,793
11,118
SE3 - 0 bar
SE3 - 1 bar
Number of Elements Passed

Fig. 6.

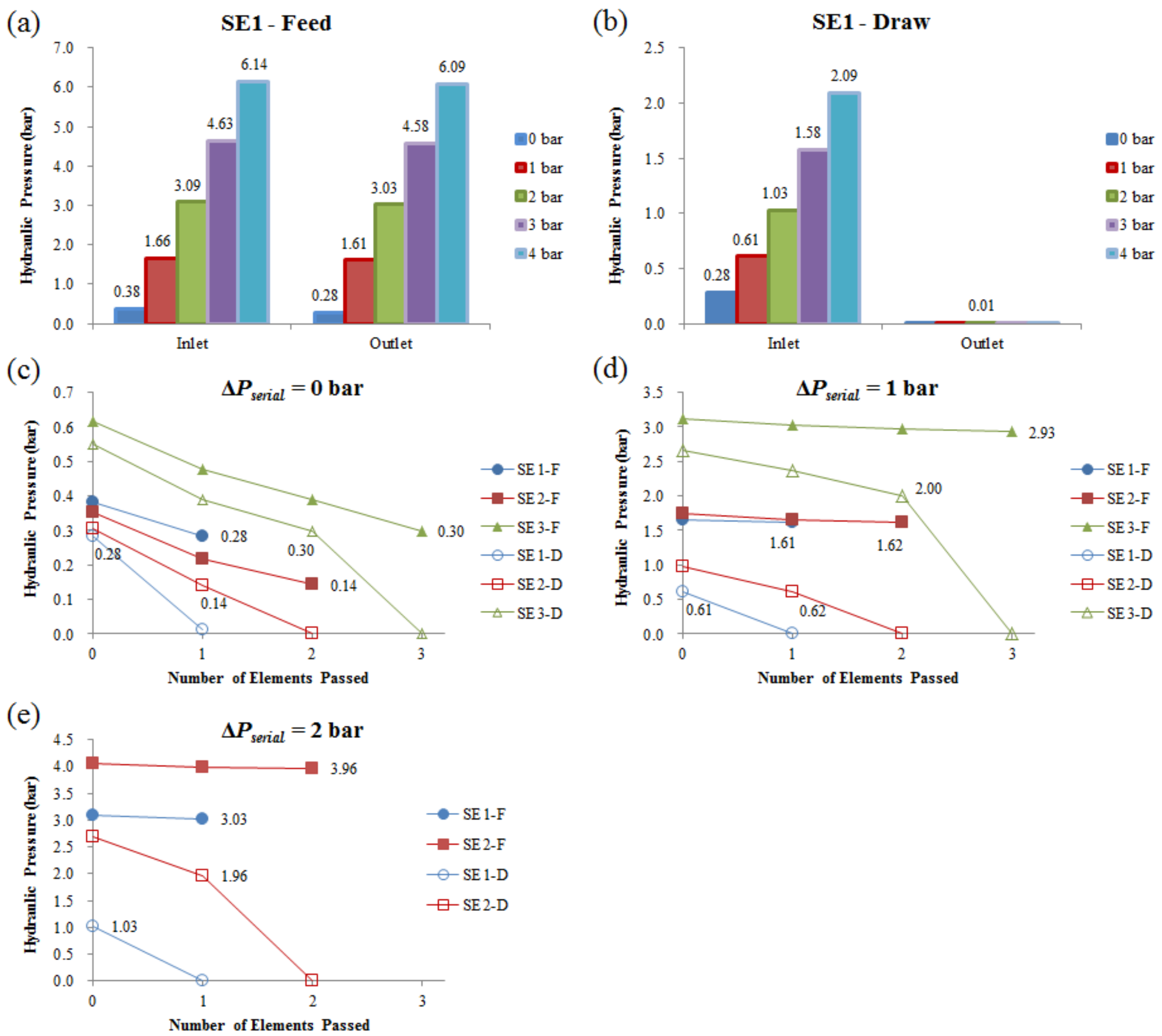

(a)
SE1 - Feed
Hydraulic Pressure (bar)
7.0
6.0
5.0
4.0
3.0
2.0
1.0
0.0
0.38
1.66
3.09
4.63
6.14
0.28
1.61
3.03
4.58
6.09
Inlet
Outlet
0 bar
1 bar
2 bar
3 bar
4 bar
(b)
SE1 - Draw
Hydraulic Pressure (bar)
2.5
2.0
1.5
1.0
0.5
0.0
0.28
0.61
1.03
1.58
2.09
0.01
Inlet
Outlet
0 bar
1 bar
2 bar
3 bar
4 bar
(c)
ΔP_{serial} = 0 bar
Hydraulic Pressure (bar)
0.28
0.28
0.30
0.14
0.14
0.30
SE1-F
SE2-F
SE3-F
SE1-D
SE2-D
SE3-D
Number of Elements Passed
(d)
ΔP_{serial} = 1 bar
Hydraulic Pressure (bar)
2.93
2.00
1.61
1.62
0.61
0.62
SE1-F
SE2-F
SE3-F
SE1-D
SE2-D
SE3-D
Number of Elements Passed
(e)
ΔP_{serial} = 2 bar
Hydraulic Pressure (bar)
3.96
3.03
1.96
1.03
SE1-F
SE2-F
SE1-D
SE2-D
Number of Elements Passed

Fig. 7.

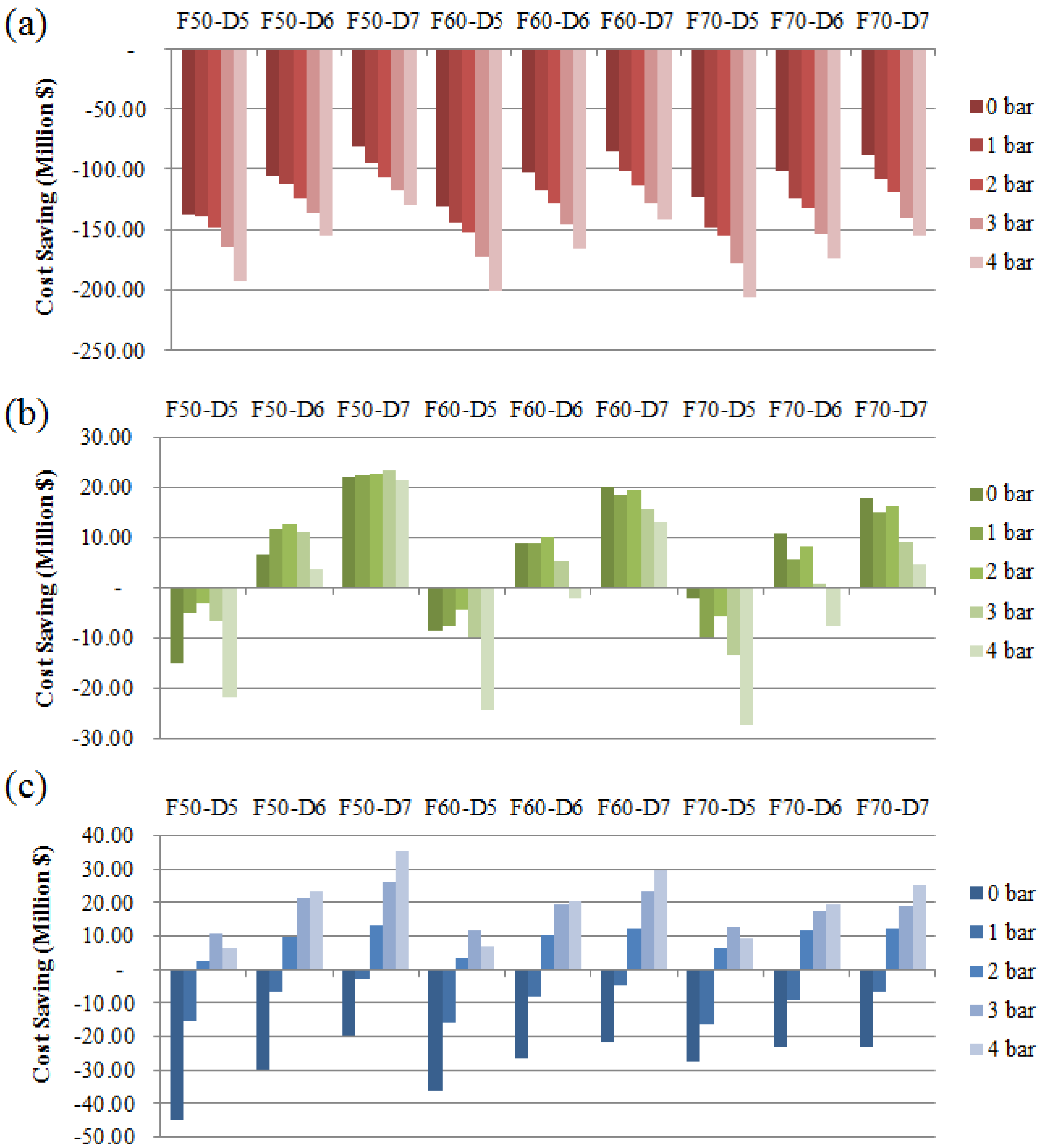
(a)
F50-D5 F50-D6 F50-D7 F60-D5 F60-D6 F60-D7 F70-D5 F70-D6 F70-D7
Cost Saving (Million $)
-
-50.00
-100.00
-150.00
-200.00
-250.00
0 bar
1 bar
2 bar
3 bar
4 bar
(b)
F50-D5 F50-D6 F50-D7 F60-D5 F60-D6 F60-D7 F70-D5 F70-D6 F70-D7
Cost Saving (Million $)
30.00
20.00
10.00
-
-10.00
-20.00
-30.00
0 bar
1 bar
2 bar
3 bar
4 bar
(c)
F50-D5 F50-D6 F50-D7 F60-D5 F60-D6 F60-D7 F70-D5 F70-D6 F70-D7
Cost Saving (Million $)
40.00
30.00
20.00
10.00
-
-10.00
-20.00
-30.00
-40.00
-50.00
0 bar
1 bar
2 bar
3 bar
4 bar

Fig. 8.

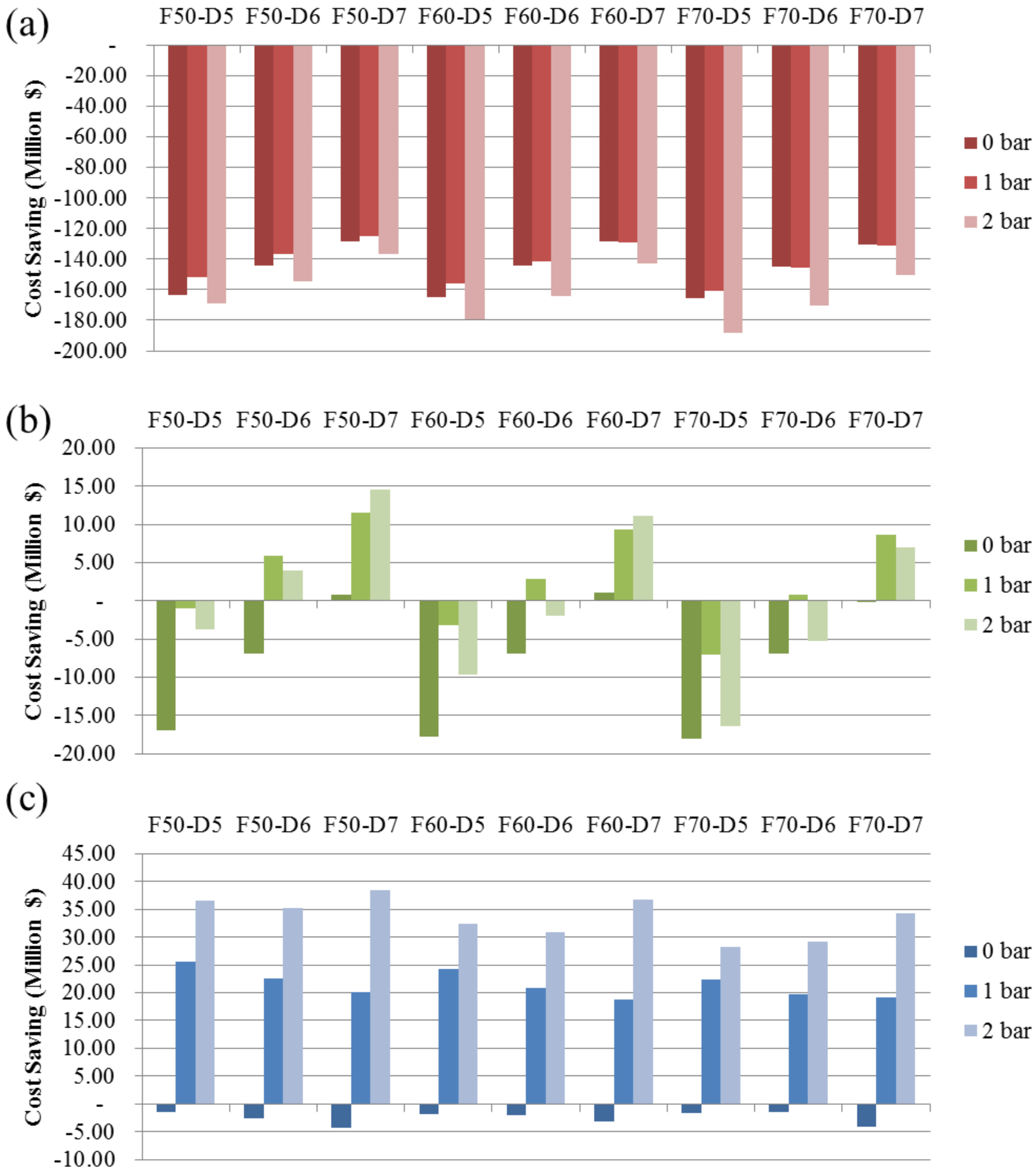
(a)
F50-D5 F50-D6 F50-D7 F60-D5 F60-D6 F60-D7 F70-D5 F70-D6 F70-D7
Cost Saving (Million $)
-
-20.00
-40.00
-60.00
-80.00
-100.00
-120.00
-140.00
-160.00
-180.00
-200.00
0 bar
1 bar
2 bar
(b)
F50-D5 F50-D6 F50-D7 F60-D5 F60-D6 F60-D7 F70-D5 F70-D6 F70-D7
Cost Saving (Million $)
20.00
15.00
10.00
5.00
-
-5.00
-10.00
-15.00
-20.00
0 bar
1 bar
2 bar
(c)
F50-D5 F50-D6 F50-D7 F60-D5 F60-D6 F60-D7 F70-D5 F70-D6 F70-D7
Cost Saving (Million $)
45.00
40.00
35.00
30.00
25.00
20.00
15.00
10.00
5.00
-
-5.00
-10.00
0 bar
1 bar
2 bar

Fig. 9.

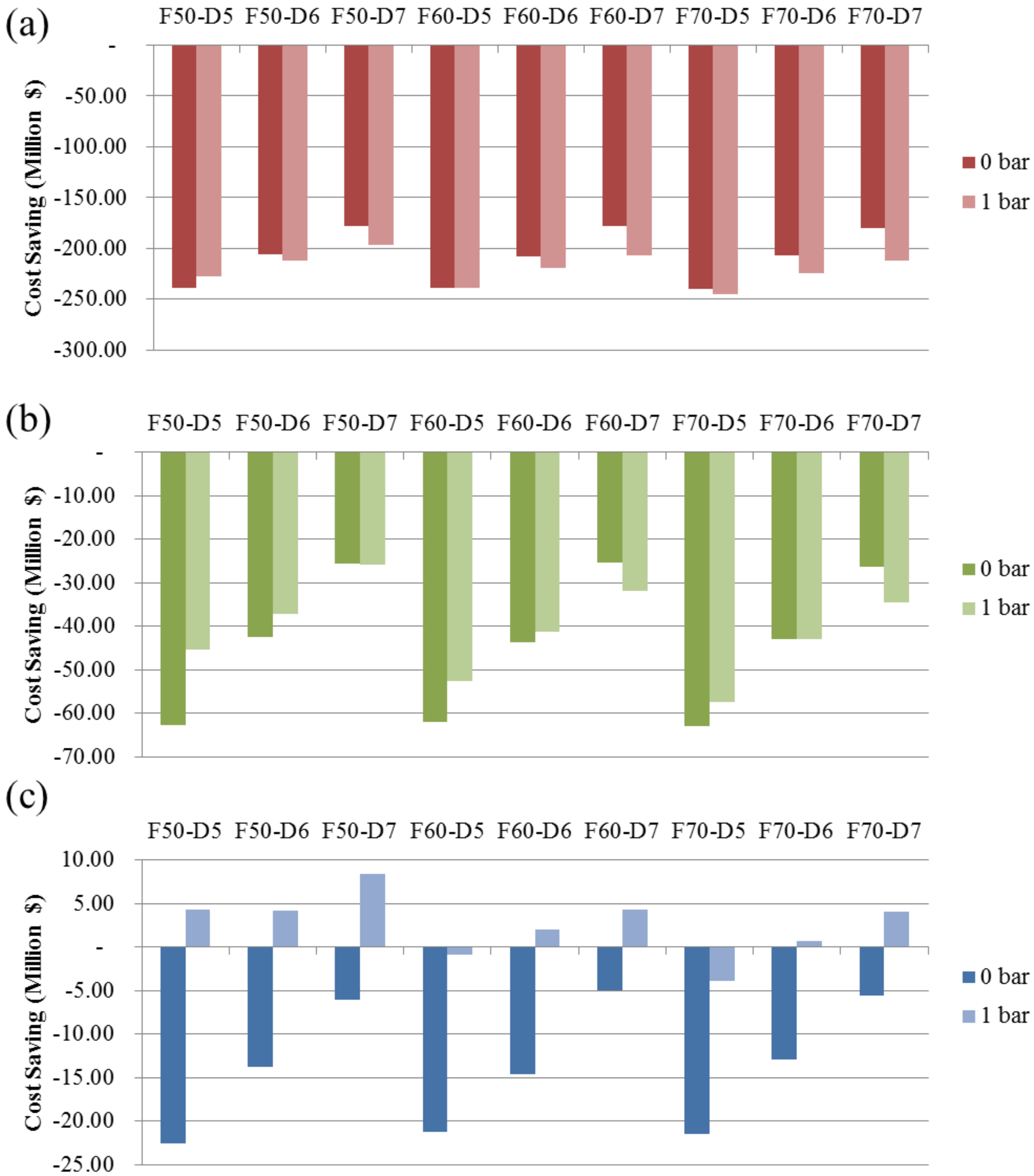

(a)
F50-D5 F50-D6 F50-D7 F60-D5 F60-D6 F60-D7 F70-D5 F70-D6 F70-D7
-
-50.00
-100.00
-150.00
-200.00
-250.00
-300.00
Cost Saving (Million $)
0 bar
1 bar
(b)
F50-D5 F50-D6 F50-D7 F60-D5 F60-D6 F60-D7 F70-D5 F70-D6 F70-D7
-
-10.00
-20.00
-30.00
-40.00
-50.00
-60.00
-70.00
Cost Saving (Million $)
0 bar
1 bar
(c)
F50-D5 F50-D6 F50-D7 F60-D5 F60-D6 F60-D7 F70-D5 F70-D6 F70-D7
10.00
5.00
-
-5.00
-10.00
-15.00
-20.00
-25.00
Cost Saving (Million $)
0 bar
1 bar

Fig. 10.

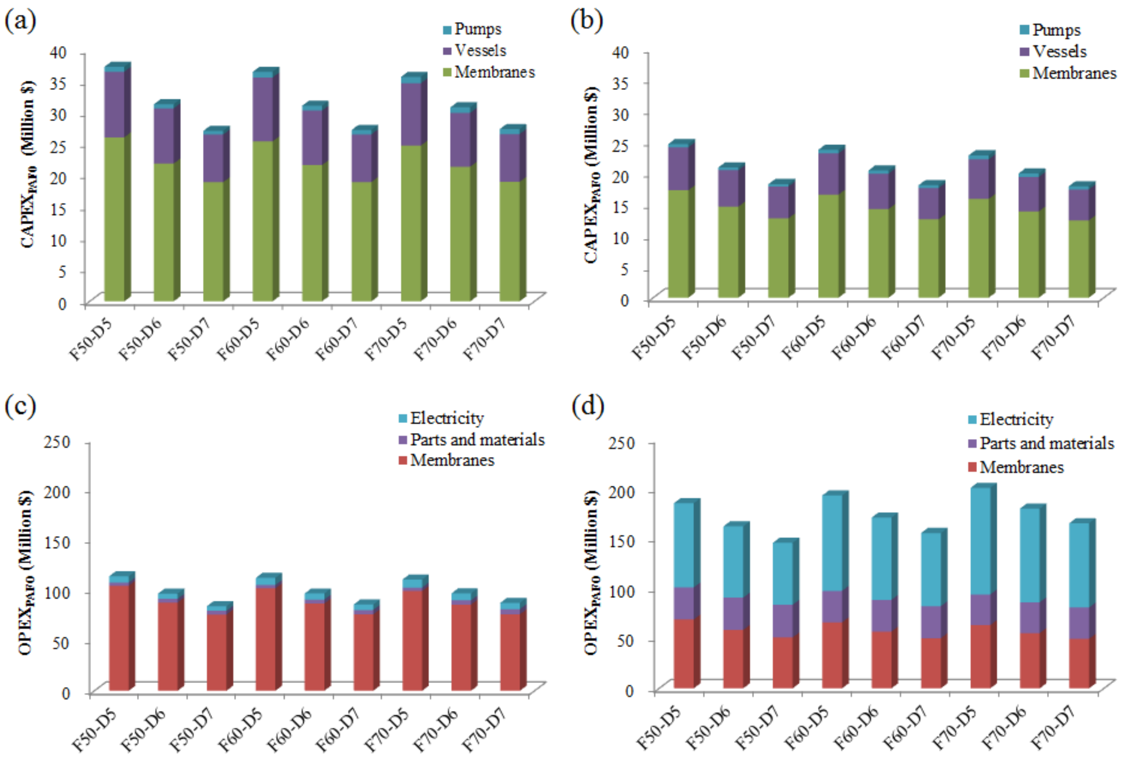

(a)
(b)
(c)
(d)
Pumps
Vessels
Membranes
Electricity
Parts and materials
$CAPEX_{PAFO}$ (Million $)
$OPEX_{PAFO}$ (Million $)
F50-D5
F50-D6
F50-D7
F60-D5
F60-D6
F60-D7
F70-D5
F70-D6
F70-D7

Fig. 11.

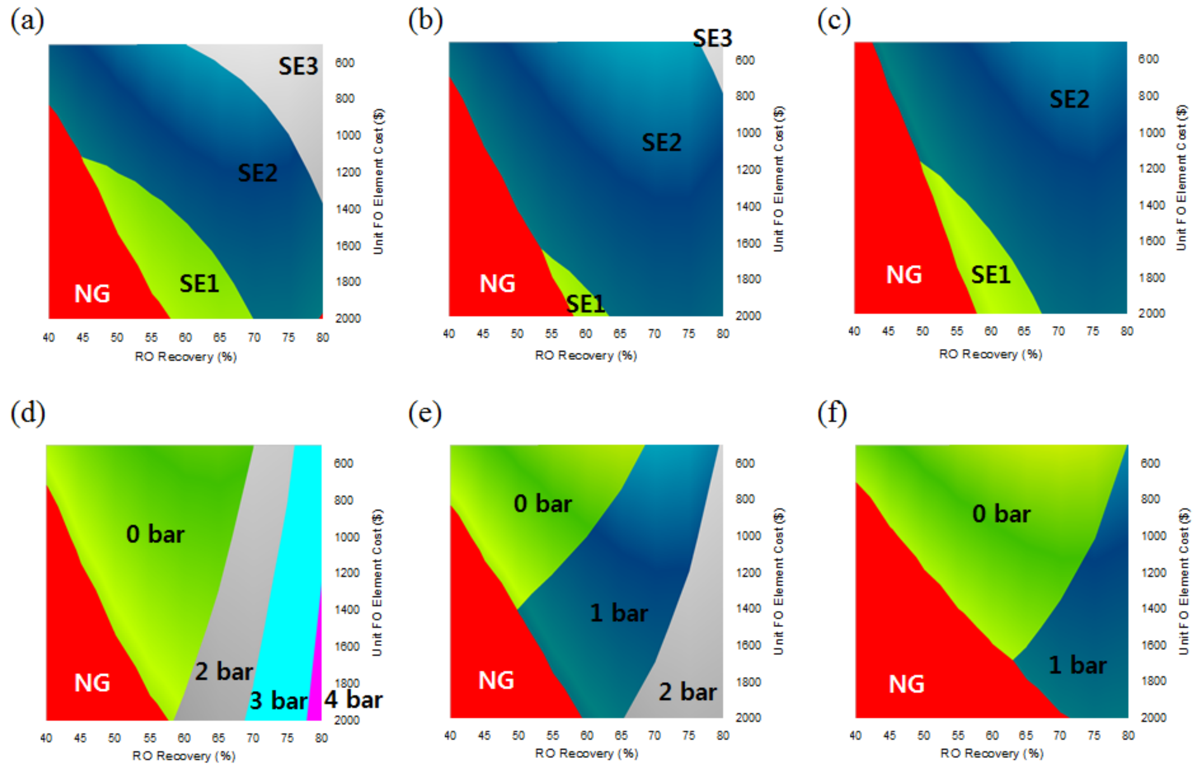

(a)
(b)
(c)
(d)
(e)
(f)
NG
SE1
SE2
SE3
0 bar
1 bar
2 bar
3 bar
4 bar
RO Recovery (%)
Unit FO Element Cost ($)

Fig. 12.

Tables

Table 1. Summary of operating conditions for pilot-scale PAFO operations

Operational Factors		Description	Note
Membrane element		CSM FO8040	Toray Chemical Korea, Inc.
Effective membrane area		15.3 m^2	For single element
Initial Solutions	Feed, $C_{F,in}$	200 mg/L TDS (500 L)	
	Draw, $C_{D,in}$	35,000 mg/L TDS (1,000 L)	NaCl (99.5% Purity, OCI, Korea)
Initial Flowrates	Feed, $Q_{F,in}$	50, 60, 70 L/min	
	Draw, $Q_{D,in}$	5, 6, 7 L/min	
Pressure Difference, ΔP_{serial}		0, 1, 2, 3, 4 bar (± 0.02 bar)	ΔP_{serial} = feed outlet pressure of the last element – draw inlet pressure of the last element
Serial Connection, SE		1, 2, 3	SE : number of FO elements in series
Temperature		25 ± 1 ºC	
Operation Time		30 min	